1994

Study of the degradation mechanisms and lifetime optimization of thin film ZnS electroluminescent devices made by MOCVD

Chongfu Yang
San Jose State University

Order Number 1359067

Study of the degradation mechanisms and lifetime optimization of thin films ZnS electroluminescent devices made by MOCVD

Yang, Chung-Fu, M.S.

San Jose State University, 1994

U·M·I
300 N. Zeeb Rd.
Ann Arbor, MI 48106

STUDY OF THE DEGRADATION MECHANISMS AND LIFETIME OPTIMIZATION OF THIN FILM ZNS ELECTROLUMINESCENT DEVICES MADE BY MOCVD

A Thesis

Presented to

The Faculty of the Department of Materials Engineering

San Jose State University

In Partial Fulfillment

of the Requirements for the Degree

Master of Science

By

Chung-Fu Yang

May, 1994

APPROVED FOR THE DEPARTMENT OF MATERIALS ENGINEERING

Dr. Emily Allen

Dr. Patrick Pizzo

Dr. Peter Gwozdz

APPROVED FOR THE UNIVERSITY

ABSTRACT

Study of the Degradation Mechanisms and Lifetime Optimization of Thin Film ZnS Electroluminescent Devices Made by MOCVD

By

Chung-Fu Yang

In order to study the degradation mechanisms of alternating current thin-film electroluminescent (AC TFEL) devices, ZnS:Mn TFEL devices prepared by metal-organic chemical vapor deposition (MOCVD) were fabricated with plasma-enhanced chemical vapor deposition (PECVD) silicon nitride films as insulating layers. The performance of these AC TFEL devices were measured. Brightness-voltage (B-V) and current-voltage (I-V) characteristics were obtained. The threshold voltage and lifetime of each working device were measured. The brightness versus operating time (B-T) characteristics were also determined. Three possible degradation mechanisms are proposed: Ag electrode delamination, dielectric breakdown, and field-induced chemical reaction. Detailed discussion on degradation mechanisms are presented as well as suggestions for future work.

ACKNOWLEDGEMENTS

I wish to express my sincere appreciation to my thesis advisor Dr. Emily Allen for her guidance, assistance, and academic professionalism combined with a clear manner of communicating throughout this work. I also wish to extend my appreciation to Dr. Patrick Pizzo and Dr. Peter Gwozdz for their assistance and advice as members of the thesis committee.

Special thanks are given to Dr. Burt Masters who gave so generously of assistance in this study; to Dr. Sree Harsha for his help on operating X-rays diffraction machine; to Dr. Evan Green for the loan of the monochromator; and to Ms. Robin King for her permission and assistance to the use of plasma-enhanced chemical vapor deposition system and other equipment in the IC lab at Stanford University.

My deepest gratitude goes to my parents for their continued understanding, encouragement and financial support of my overseas study. The support obtained from my brothers is warmly acknowledged.

Finally, I wish to thank my cousin, Yueh-Lee Young, and her family for providing me a room and tolerating the inconvenience I may have caused during the writing of the thesis.

TABLE OF CONTENTS

LIST OF TABLES

LIST OF FIGURES

1. INTRODUCTION

1.1.Overview of Electroluminescent Devices

Electroluminescence (EL) is the emission of light from a material solely due to the application of an electric field. In principle, to construct such a lamp or an information display is quite simple. However, the completion of a practical display using the basic phenomenon has been studied by the industry for many years. Thin film electroluminescent devices have been successfully fabricated at the Materials Engineering Thin-Film laboratory at San Jose State University by Chuang.[1] The typical brightness-voltage (B-V) and current-voltage (I-V) characteristics were observed. The threshold voltage was in the range of 100 to 220 rms volts. However, the poor reproducibility in performance of the TFEL devices needed to be improved as did the short lifetime problems. The present work was conducted in an effort to alleviate these problems, improve the fabrication process, and study the degradation mechanisms.

In this chapter, the purpose, history and the development of EL devices are reviewed, as well as the flat panel display technology. Since the explanation of the exact mechanisms for light generation is now reasonably well understood, the theories of EL generation will be discussed

in Chapter 2. Still in Chapter 2, the theories of insulating layers in thin-film electroluminescent displays will be presented. In Chapter 3, the preparation of the light emitting region, ZnS:Mn, will be considered in terms of different fabrication techniques. The detailed procedures of fabricating EL devices will be presented in Chapter 4. The experimental results and discussion in this work will be shown in Chapter 5. Finally, Chapter 6 will conclude the entire work. The information about the modification of MOCVD system are included in the Appendices.

Electroluminescence in phosphors was discovered by Destriau in 1936.[2] EL was recognized as a new physical phenomenon that produces light by exposing phosphor materials to high electric fields. He was working with a popular photoluminescent phosphor, ZnS activated with Cu, and by accident observed that light was emitted solely because of the application of an electric field. Due to the immaturity in the fabrication techniques of transparent electrically conductive films, EL was not developed at once after Destriau's publication. No positive effort was made in developing the phenomenon into a practical device until the 1960s. During that period, most work concentrated on the dispersion type ac powered EL device which consisted of activated phosphor powder dispersed in an insulating layer,

with the expectation that it would turn out to be a new light source for wall illumination. A number of devices were manufactured around 1960, but the low luminance, short useful operating lifetime, poor visibility in normal room light, and lack of visibility under high ambient light were barriers which needed to be overcome.[3,4] Those problems were mainly solved by the invention of the Lumocen device[5] in which a vacuum-deposited thin phosphor film replaces the dispersion layer structure. It consisted of SnO_2 (200 nm), HfO_2 (300 nm), ZnS:TbF_3 (150 nm) and an Al electrode, all on a glass substrate. Operating devices were demonstrated, but the life was short.

In 1974, Sharp Corporation demonstrated a 240 by 320-line thin-film electroluminescent monochromatic TV for the first time in EL development history, using electron-beam evaporation of the ZnS:Mn and applied better insulators. They also presented two papers at the 1974 Society of Information Display (SID) international symposium.[6,7] They showed that they have fabricated long life devices of 10^4 hours, with brightness of 10^3 fL. Soon after the Sharp disclosures, EL display devices were once more being researched and developed by high-technology companies. The vacuum-deposited thin film EL device with a double insulating structure not only exhibits high brightness, stability and long life, but it can also be processed to possess inherent memory which gives

itself to very wide applications.

After the success of monochrome thin film electroluminescence an intensive search began for other colors than the yellow of ZnS:Mn. ZnS as well as other hosts, especially alkaline-earth sulfides, such as SrS[8,9,10], CaS[11,12] II-VI compounds doped with various rare-earth ions which cover a wide variety of wavelengths in the visible spectrum, have been extensively investigated. It is well known that lanthanide rare-earth ions show a wide variety of emissions which cover the ultraviolet (UV) to infrared regions because of the internal transitions by the 4f electrons or 4f-5d transitions.[13] The II-VII_2 compounds were also investigated as the EL phosphor material. CaF_2:Eu thin film EL devices were reported to emit blue light.[14] Orange-emitting ZnF_2:Mn thin film EL devices were reported by Morton and Williams.[15]

In recent years, EL has been well developed and thought a promising means for flat information display devices. A discussion of current techniques for making flat panel displays including liquid crystal display and thin-film electroluminescent display will be presented in the next section.

1.2.Flat Panel Display Technology

Applications of flat panel displays (FPDs) for laptop computer and TV receivers have been rapidly researched and developed over the years.[16,17] Due to their characteristics of low volume and light weight, flat panel displays have become the center of attention in computer and TV manufacturing. Many kinds of techniques are used for making FPD, including liquid crystal display (LCD), gas-plasma display, alternating current thin film electroluminescent (ACTFEL) display, vacuum flourescent display (VFD), light emitting diode (LED), flat cathode ray tube, and electrochromic display. Each of those has its own specific application.

Three major FPD display techniques, gas-plasma, LCD and TFEL, have been developed and revolutionized computers, televisions, household appliances, medical equipment, military equipment and other devices that need to display text or graphics.

LCDs provide many advantages, for instance, small size, light weight, low power consumption, and good resolution (typically 640 by 480 pixels). Currently, active-matrix or thin-film transistor (TFT) LCD have primarily been produced for small size full-color TVs.[16,17] Gas-plasma displays

operate by exciting gas, usually neon or an argon-neon mixture, through the application of a voltage. By applying sufficient voltage at an addressed matrix intersection, the gas is excited, emitting an orange-red light. Gas-plasma displays have faced many problems. Their lack of full-color capabilities, their relatively short life span, and their cost have all contributed to their slow emergence.[16]

TFEL displays work on the principle of electroluminescent-phosphors emitting light in the application of an alternating electrical field. EL displays are becoming popular in military and industrial applications requiring portability and reliability in hostile environments.[18] TFEL displays range in size from 2 by 2 inches to 12 by 14 inches, with resolutions ranging from 320 by 128 pixels to 640 by 400 pixels. TFEL displays offer better contrast and broader viewing angles than LCDs but less than gas-plasma and cathode ray tubes (CRTs).[19] The main problem in TFEL market acceptance has been its price. To overcome this problem, the costs of production of TFEL displays, such as ICs, circuit board, and other materials used in its fabrication, have to be reduced in order to commericalize the products. Table 1. summarizes the advantages and disadvantages of alternating current thin film electroluminescent (ACTFEL) displays and LCD techniques.

Table 1. Comparisions of advantages and disadvantages of ACTFEL displays and LCDs.

	Advantages	Disadvantages
ACTFEL	High constrast Broad viewing angle Good resolution Fast response time Full-color capability Large-area display	More power consumption High cost
LCD	Low power consumption Good resolution Small-area display Light weight Full-color capability	Narrow viewing angle Slow response time Small-size display

2. THEORY OF OPERATION

2.1. Structure of Thin Film Electroluminescent (TFEL) Devices

The fundamental form of the ac TFEL structure is shown in Figure 1. It consists of a glass substrate and five thin-film layers. The front electrode is a transparent conductor such as indium-tin oxide (ITO). The next three layers consist of the phosphor, ZnS:Mn, sandwiched between two insulating layers. The top layer, in Figure 1, called the back electrode, is often reflective aluminum. When a source of alternating voltage is applied to the electrodes, no light is emitted as long as the applied voltage is less than the device threshold voltage. When the applied voltage exceeds the threshold value, electroluminescence is observed through the transparent electrode.

As described in Figure 1, ACTFEL devices normally use a completely symmetric structure of two insulator layers (I) between which the active semiconductor layer (S) is embedded. Contacts (M) for applying the ac voltage are provided on the outer surfaces of this (ISI) structure. This structure is also called the metal-insulator-semiconductor-insulator-metal (MISIM) structure. Because of this sandwich structure,

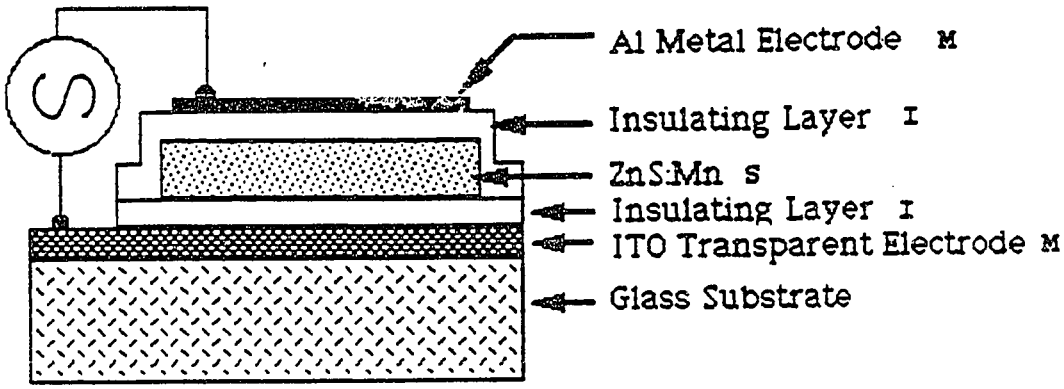

Figure 1. Schematic structure of an ac thin film electroluminescent device.

undesirable leakage current flowing through the device is effectively prohibited. Consequently, the device can contain a high electric field for EL operation across the active layer without breakdown. The required properties of each layer are described below.

Front Electrode: The front electrode must be very conductive and as transparent as possible so that the emitted light will not be blocked. The best front electrode has been found to be indium-tin oxide (ITO)[20], In_2O_3:SnO_2, which is a transition metal oxide semiconductor with sheet resistance of approximately 5 ohms per square and a transparency of 80%. A restriction related to reliability is that the transparent electrode has to be free of asperities which may cause electric field enhancements or pinholes in the thin insulator. Thickness uniformity must also be retained if optical interference colors are to be avoided. Conductivity, surface smoothness and thickness uniformity become increasingly important as the physical size of the display increases.

Insulating Layer: The importance of the insulating layers cannot be overemphasized. The function of the insulating layer is simple. It has to stabilize any possible electrical breakdown of the semiconductor layer by its high resistivity. For most devices, insulator reliability

determines the device reliability. Furthermore, its parameters influence the operating voltage, the capacitive load, the maximum luminance, and the need for additional encapsulation.[21] These aspects will be discussed in detail in section 2.4.

Semiconductor Layer: The semiconductor layer (or host) contains the luminescent centers which are to be electrically excited. This excitation, discussed in the next section, is achieved by direct impact of carriers (electrons) highly accelerated by the electric field. This process was first discussed by Cusano[22], and experimentally proved by Krupka.[23] Thus the functions of the semiconductor layer are to contain the emitting centers and to provide the "hot" electrons that will be definited in the next section.

The host should have enough surplus of gap energy over the Mn-excitation energy of about 2.5 eV in order to have some space for the hot carrier energy in between excitation of the center and impact ionization of the lattice. This excitation will be seen in Figure 3 in section 2.2. The most suitable host material for the luminescent center Mn is ZnS because of its wide band gap, 3.66 eV, and brightness considerations. Electroluminescence has also been obtained in ZnSe[24], ZnF_2[25], and CdF_2[26] with Mn as luminescent centers. However, none of these gave as high brightness as

ZnS. Thus, ZnS will be used in this study.

Another interesting feature of the ZnS:Mn system is that it exhibits hysteretic or memory effect. This effect will be discussed in detail in section 2.3, but basically hysteretic behavior refers to a multilevel light output stability at the same applied voltage amplitude. This property can be developed to control the contrast of TFEL displays for a grey scale.[27]

Luminescent Center: The function of introducing dopants into the host as luminescent centers is to provide a center where hot electrons can impact-excite the dopants and then generate electroluminescence by releasing energy from the dopants. Therefore, for a suitable luminescent center the main requirements are[28]:

(1) Large cross section in order to increase the probability of impact excitation.

(2) High solubility in the host in order to enhance the efficiency of impact excitation by hot electrons.

(3) Inner shell transitions, well shielded against electric fields to prevent possibility of the ionization of luminescent center under high field excitation.

(4) Emission in the visible light range.

Fortunately, there is one dopant which almost satisfies all reqirements. That element is manganese (Mn). However, it only provides one color (yellow). Other colors can be achieved by using rare-earth ions. The yellow light is emitted as the Mn ion relaxes from an excited state in the ZnS:Mn devices. For Mn activator, the $^4T_1(^4G)$-$^6A_1(^6S)$ transition is believed to be responsible for the yellow light as shown in Figure 2.

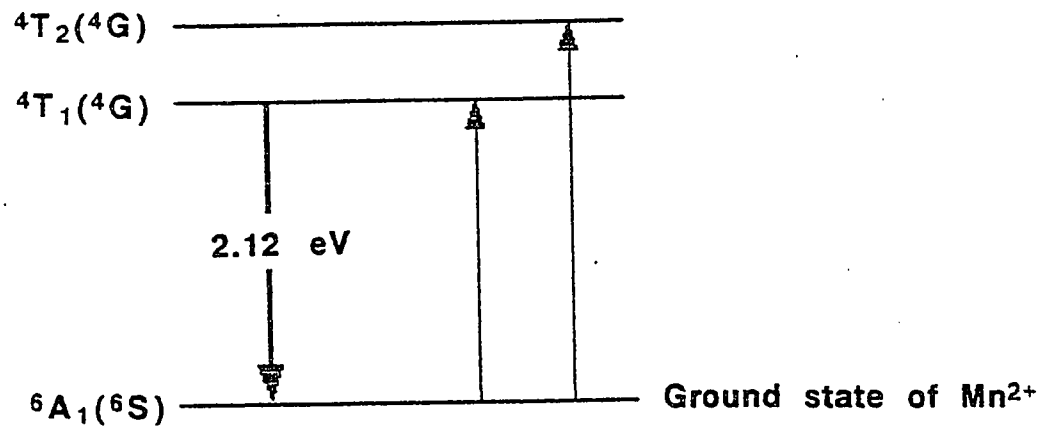

Figure 2. Two energy bands showing the Mn transitions responsible for the yellow light.

Back Electrode: The top layer in TFEL devices, called the back electrode, is usually reflective aluminum. The aluminum electrode can survive better than other electrodes because it fuses to an open circuit in the immediate vicinity of any pinhole breakdown that may occur. The aluminum electrode thickness is often made about 20 to 50 nm.[29]

2.2.Electroluminescence Generation Mechanisms

Most luminescence processes involve three major steps: first energy absorption, then the local center excitation, and finally energy emission in the form of radiation with wavelength in the visible range of the spectrum.

Direct impact excitation of a luminescence center by hot electrons is thought to be the dominant excitation mechanism in a thin film electroluminescent device. Evidence for direct impact excitation was first proposed by Krupka[23] of Bell Telephone Laboratories, on rare-earth doped ZnS thin films and by Tanaka et al.[30], on ZnS:Mn thin films. The following energy band diagram of a TFEL device with the MISIM structure shown in Figure 3 [31] is based on using ZnS as the phosphor layer with Mn as the luminescent center, the best combination in the ac thin film configuration.

Figure 3 schematically presents the mechanisms of an ac

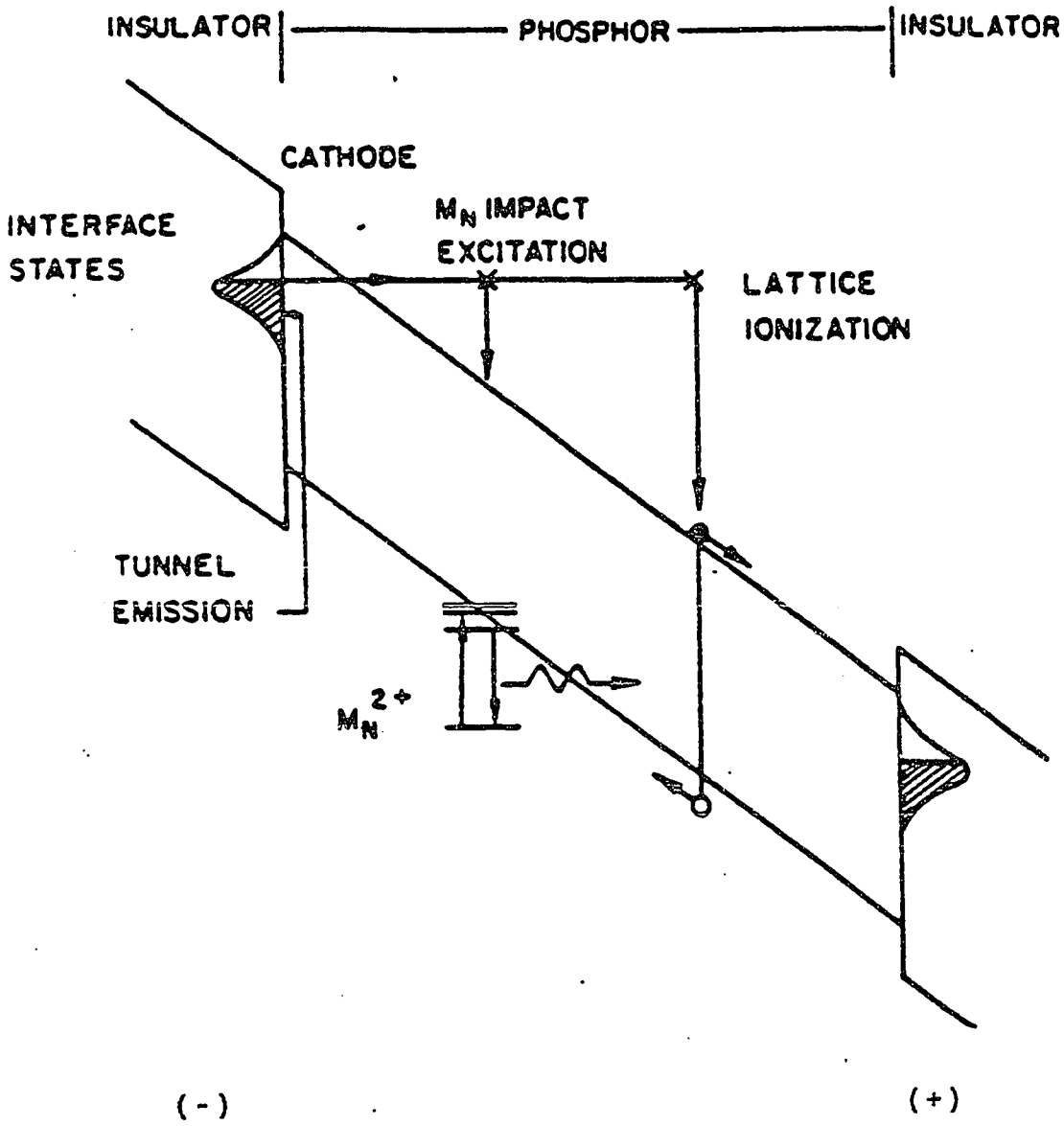

Figure 3. Band diagram illustrating some of the important mechanisms in an ac TFEL device under applied voltage.[31]

TFEL device with the energy band diagram. Only the phosphor layer and the interface to the adjacent insulating layers are shown here. The simplest description of the mechanism of ac TFEL displays can be briefly concluded as the following basic processes.

When one applies a bias field on the electrodes of a TFEL device, a temporary cathode, as illustrated in Figure 3, on the left-hand phosphor-insulator interface occurs. Electrons located at the phosphor-insulator interfaces next to the temporary cathode are tunnel-emitted into the conduction band of the phosphor. Then, these electrons are subsequently accelerated by the applied electric field in the conduction band of ZnS. These electrons are so-called hot electrons. When these hot electrons gain enough energy from electric field, they can impact-excite the $3d^5$ electron of Mn^{2+} luminescent centers which will quickly return to their ground states and release energy in form of radiation. This generated light is called electroluminescence. Moreover, some of the energetic electrons can also impact-ionize valence band electrons of ZnS, creating electron-hole pairs. Positive space charge generated by lattice ionization will be accumulated in the bulk. However, electrons, after being multiplied by impact ionization, will travel to the right-hand side, the temporary anode, and are trapped in the interface between the insulator and the phosphor layer. When

the polarity of this interface is reversed, these electrons are again tunnel-emitted and transported to the conduction band of phosphor and repeat the process.

From above discussion, there is a threshold behavior involved in these processes. Apparently, in order to perform a tunnel emission of interface trapped electrons, a threshold field strength at the temporary cathode interface is required. This value is dependent upon the energy distribution of the interface trapped electrons and on the amount of charge trapped in the interface. Generally, the electron interface state density is fairly high in these ac TFEL devices. Typically, up to some 10^{13} electrons/cm^2[32] are transferred in every excitation pulse. This subject is given more detailed discussion in terms of a expression for the current **J** of electrons tunnel-emitted from a distribution of interface states under applied electric field as follows.

Electrons trapped in energy levels in the band gap at the cathodic phosphor-insulator interface can tunnel through the energy barrier. The width of this barrier is inversely proportional to the electric field in the phosphor layer, shown in Figure 4.[32] We can write a expression for the current **J** of electrons tunneling from a distribution of interface states under the field E in the following form.

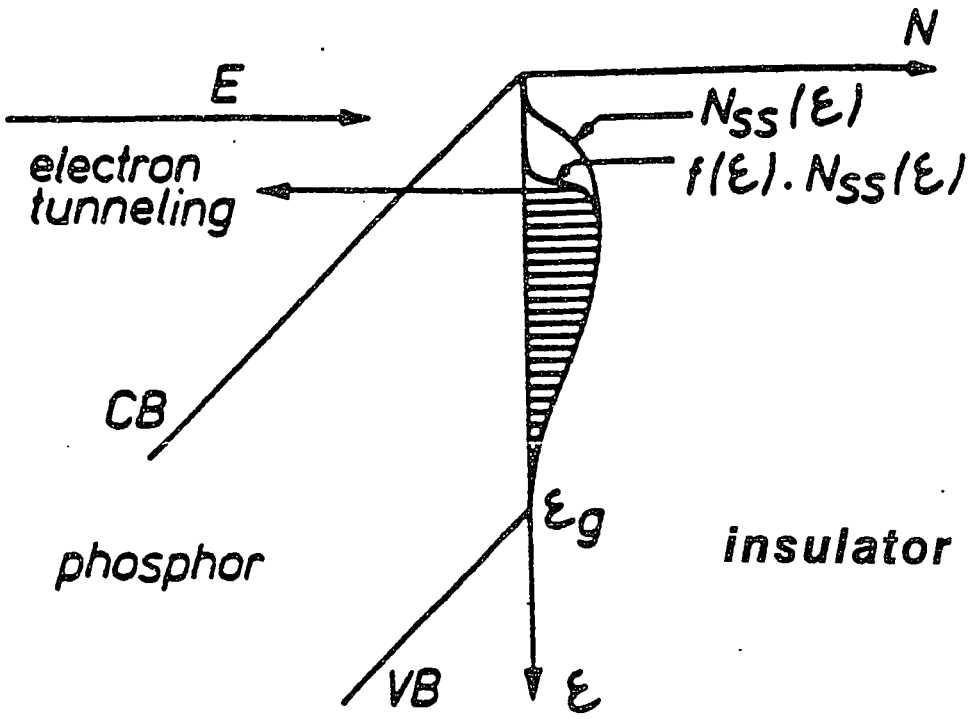

Figure 4. Tunneling mechanism from the phosphor-insulator interface states of ac TFEL devices.[32]

$$J_{\cdot} = \int_0^{\epsilon_g} q f(\epsilon) N_{ss}(\epsilon) \Phi \exp\left(-\frac{\epsilon^{3/2}}{BE}\right) d\epsilon, \qquad (1)$$

where q is the electron charge, B is a constant, ε is the energy depth of the interface state, ε_g is the band gap energy, $N_{ss}(\varepsilon)$ is the density of interface states measured in number per cm^{-2} per eV, $f(\varepsilon)$ describes the occupancy of these states, and Φ is a slowly varying function of E and ε. From this expression, we can know that for a given phosphor and electric field, the characteristics of the tunnel emission are controlled by parameters closely related to the chemistry and morphology of the interface, such as ε, $N_{ss}(\varepsilon)$, and $f(\varepsilon)$. That is, it depends on which insulator is used and how it is deposited. Figure 3 also illustrates the distribution of interface states and main processes discussed here.

2.3.Aging and Memory Effect

A well-known phenomenon in brightness-voltage characterictic is the shifting of threshold voltage. This phenomenon will be shown later in the "Results and Discussion" section. The shift of the threshold voltage to higher values with operation seems to be unavoidable in triple layer TFEL devices, consisting of ZnS:Mn active layer sandwiched by a pair of insulating layers. However, some researchers have proposed new TFEL structures to reduce

the shifting behavior. A new TFEL structure with PSG (phospho-silicate glass) film between the interface of phosphor and insulator to suppress the shifting in B-V characteristics has been proposed, but sufficient result has not been acquired.[33] Another new TFEL structure was suggested by using a CaS thin film as a buffer layer between the interface of phosphor and insulator.[34] Although the effect of buffer is not yet clear, the shifting in B-V characteristics can be reduced by simply depositing this thin buffer layer.

Another interesting brightness-voltage characteristic in TFEL devices is the hysteretic or memory effect. Memory effect is belived to be due to the storage of space charge at the phosphor-insulator interface areas during power application, thus forming an internal field which adds to the external field on voltage reversal, resulting in enhanced light emission.[35,36,37]

As shown in Figure 3, space charge formed by impact of hot electrons will be trapped and build up at the phosphor-insulator interfaces, resulting in a localized field enhancement. When the applied voltage decreases, the charge stored at the phosphor-insulator interfaces adds to the internal electric field applied to the phosphor, leading to a further enhancement of current flow even when the applied

voltage is below threshold voltage. This addition of stored charge is the reason causing the bistability behavior in ac TFEL devices during the reversal of applied voltage. More detailed theory discussion has been studied and written in Chuang's thesis.[1]

2.4.Theory of Insulating Layers in TFEL Devices

2.4.1.Ideal Model and High Brightness TFEL Devices Design

An ac thin-film electroluminescent (TFEL) device, as initially made by Inoguchi et al.[6] in 1974, makes use of an insulating layer adjacent to the active layer to limit the amount of charge which can flow through a given area of the device per voltage reversal. They developed a high-brightness long-lived TFEL device fabricated from ZnS film doped with Mn, sandwiched between two yttrium oxide (Y_2O_3) insulating layers. Even though the device exhibited a high brightness about 1500 fL (=5200 cd/cm^2) at 5 kHz ac 250 V and long life, it required a fairly high operating voltage. Therefore, lowering the driving voltage below 100 V has been one of the important problems to solve in making a practical flat panel display with low power dissipation as well as the possibility of large-area fabrication.

To appreciate the insulator requirements from the device physics point of view, it is important to understand the impact excitation mechanism. From previous discussion in section 2.2, the electrons used for impact excitation are located at the phosphor-insulator interfaces. The energy distribution of these interface states determines the energy distribution of the electrons and the device performance. It has been experimentally verified[38] that insulating materials that have large bandgaps and deep interface states result in higher brightness than insulators that provide numerous shallow states. In addition, the insulators must maintain the stored interface charge at high fields and not leak it. Howard[21] was the first to give a rule of thumb for the figure of merit of an insulator for TFEL displays. The rule says the charge storage capacity at breakdown should be at least three times that of the active layer of the device. From this basis, a value in excess of 3 $\mu c/cm^2$ is often required for charge storage capacity.

In order to design a TFEL device with optimum insulators, it is helpful to consider a simple series capacitor model, such as the "ideal model" described by Alt[31]. The following discussion is based on Alt's model. In this model, the phosphor is assumed to be insulating below the threshold field for light emission. The sandwich structure, consisting of the phosphor and two insulating

layers, can be modeled as three capacitors in series as shown in Figure 5 (a). The equivalent circuit of such an ac-coupled TFEL device is shown in Figure 5 (b).

During light emission charge flow through the phosphor is controlled by the cathode field. Assuming the field is controlled only by the voltage across the phosphor, a voltage-controlled current source in parallel with the phosphor capacitance represents this effect. The current source is defined as an abrupt transition from zero current to an arbitarily large value; the transition point is called the threshold voltage. This behavior is illustrated in Figure 5 (c). The light produced is assumed proportional to the charge transported times the threshold voltage, that is, to energy dissipated in the phosphor. The proportionality constant is the luminous efficiency η. This relationship will be derived through the following steps, and shown in equation (16).

The symbols used in this section for equation derivations are defined and summarized as follows:

- η is the luminous efficiency,
- C_I is the insulator capacitance per unit area and is equal to ε_I / t_I,
- C_Z is the ZnS capacitance,

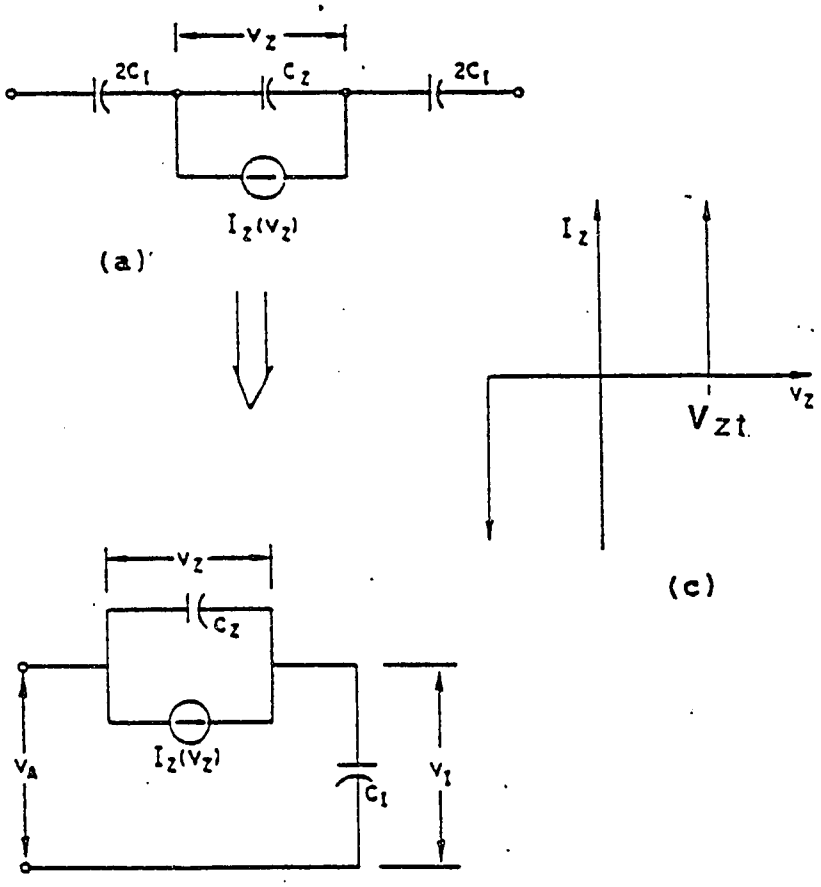

Figure 5. Ideal model for a double insulated ac TFEL device. (a) Ideal capacitor model of the sandwich structure. (b) Ideal model equivalent circuit of an ac-coupled TFEL device. (c) Definition of the threshold voltage.[21]

V_A is the applied voltage,

V_Z is the voltage across the ZnS,

V_I is the voltage across the insulator,

V_{Zi} is the initial voltage across the ZnS,

V_{Ii} is the initial voltage across the insulator,

E_{Zt} is the threshold field in the phosphor,

V_{Zt} is the $E_{Zt} \cdot t_Z$, threshold voltage across the ZnS phosphor,

t is the thickness,

ε is the dielectric constant.

From above point of view, the applied voltage is equal to the sum of the voltages across the insulator and phosphor, that is,

$$V_A = V_Z + V_I. \qquad (2)$$

The subscript Z refers to ZnS phosphor, and I refers to the insulator. When the applied voltage is pulsed or sinusoidally swept through the device, only a limited amount of charge per unit area can pass through the ZnS film, depending upon the capacitance of the insulating layer. Initially, the voltage is capacitively divided, so that,

$$V_{Zi} = \frac{C_I}{C_I + C_Z} V_A, \tag{3}$$

$$V_{Ii} = \frac{C_Z}{C_I + C_Z} V_A. \tag{4}$$

If V_{Zi} is above the threshold voltage, V_{Zt}, charge will flow transiently through the phosphor producing light, and charge up the insulator capacitance until the voltage across the phosphor is reduced to its threshold value. So, the final values are

$$V_{Zf} = V_{Zt}, \tag{5}$$

$$V_{If} = V_A - V_{Zt}. \tag{6}$$

The voltage transferred, from the phosphor to the insulator capacitance, is then given by

$$\Delta V = V_{If} - V_{Ii} = V_{Zi} - V_{Zf}, \tag{7}$$

$$\Delta V = V_{Zi} - V_{Zt}. \qquad (8)$$

Or, in terms of the external threshold voltage, V_{At},

$$\Delta V = \frac{C_I}{C_I + C_Z} (V_A - V_{At}). \qquad (9)$$

The corresponding charge transferred is

$$\Delta Q = C_I (V_A - V_{At}) = \int I_Z \, dt. \qquad (10)$$

If a second pulse of the same amplitude and polarity is applied, the intial voltage across the phosphor this time is

$$V_{Zi} = V_A - V_{I(previous)}$$
$$= V_A - (V_A - V_{Zt}) = V_{Zi}$$

Thus, no conduction takes place and no light is emitted. The corresponding waveforms for these two pulses are given in Figure 6.

If a pulse of the same amplitude and opposite polarity, pulse P3 in Figure 6, is now applied, and if the charge at the interface, Q, has not decayed, then the initial and final voltages across the phosphor are

$$V_{Zi} = \frac{Q}{C_I + C_Z} + \frac{C_I}{C_I + C_Z} V_A, \qquad (11)$$

$$V_{Zf} = V_{Zt} = \frac{C_I}{C_I + C_Z} V_{At}, \qquad (12)$$

and the transferred voltage for pulse 3 is

$$\Delta V_3 = 2 \frac{C_I}{C_I + C_Z} (V_A - V_{At}), \qquad (13)$$

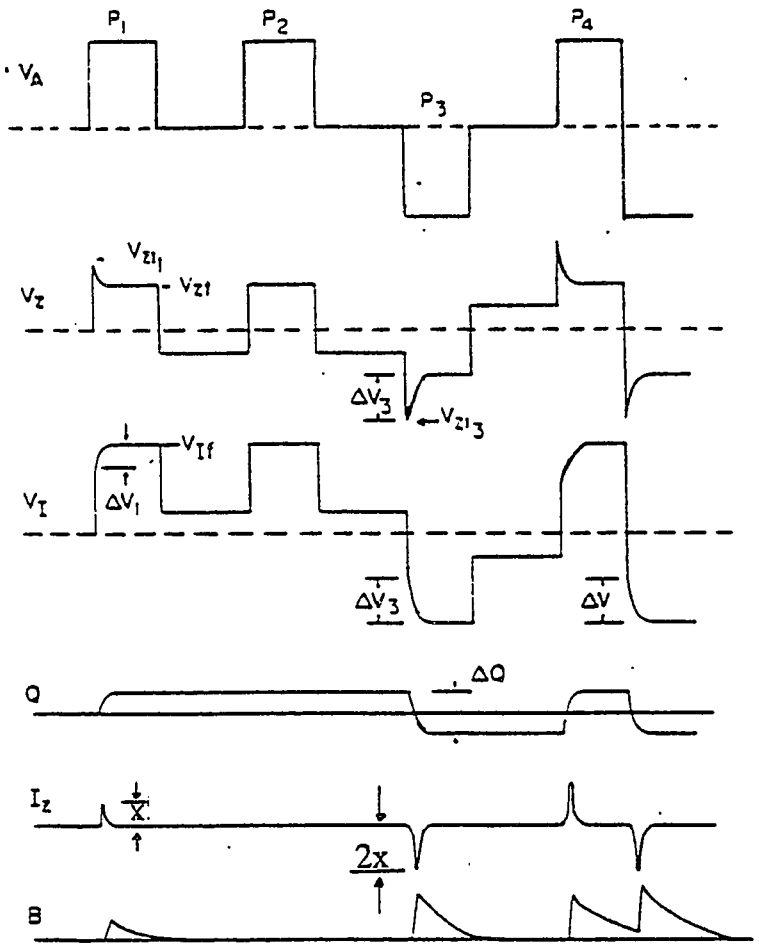

Figure 6. Waveforms indicating a particular pulse excitation sequence and the resulting changes in internal voltage, charge, current and emitted light. The equivalent circuit of Figure 5 is assumed.[31]

or twice the value for the first pulse. Succeeding pulses of alternating polarity will also transfer this amount. In the steady state, the interface charge at the end of a voltage pulse is one-half the transferred charge; one-half the transferred charge neutralizes the previous charge, and the remaining half replaces it with an equal amount of opposite polarity. For steady-state, square-wave excitation, the voltage and charge transfer are respectively;

$$\Delta V = 2 \frac{C_I}{C_I + C_Z} (V_A - V_{At}), \qquad (14)$$

$$\Delta Q = 2 C_I (V_A - V_{At}), \qquad (15)$$

Therefore, the total light output L, assumed to be proportional to the product of charge transported through and the voltage across the ZnS phosphor, is

$$L = 2 \eta C_I V_{Zt} (V_A - V_{At}), \qquad (16)$$

and the threshold voltage V_{At} is given by the following equation:

$$V_{At} = E_{Zt} \left(t_Z + t_I \cdot \varepsilon_Z / \varepsilon_I \right). \qquad (17)$$

Equation (16) can be reduced to

$$L \propto \varepsilon_I \cdot t_Z / t_I \qquad (18)$$

From Eq.(17) and (18), it is obvious that for high brightness and no increase in threshold voltage, t_Z / t_I and ε_I must be as made as large as possible. In order to maintain V_{At} unchanged, any increase in threshold voltage due to an increase in t_Z must be canceled by a decrease in V_{At} due to larger ε_I / t_I values. In practice, the safety margin of the device (defined as the ratio of breakdown voltage to threshold voltage), which is proportional to C_I / C_Z, must have a large value. Thus, to design a high brightness TFEL device can be simply achieved from this ideal model by considering the dielectric constant of the insulator and the thickness of the insulator and phosphor.

However, for a practical device fabrication, the thickness uniformity and homogeneity of each layer, and the particle-control process must also be taken into account.

Therefore, for a practical design, a compromise must be made based on actual defect levels, process technology, etc. The TFEL fabrication techniques will be discussed in Chapter 3. The following section presents the common insulating materials used in AC TFEL displays.

2.4.2.Choice of Insulating Layer for TFEL Devices

From the safety consideration point of view, in a double insulator TFEL display, insulating layers that provide maximum protection against electrical breakdowns with minimum voltage drop must be used. Therefore, in order to minimize the voltage drop, high dielectric capacitances are needed. Another insulator parameter crucial to device operation is the maximum charge storage capacity, Q_{max}, that is, the density of charge stored just before breakdown. It can be indicated as

$$Q_{max} = \varepsilon_I \bullet E_{BD} \qquad (19)$$

where ε_I is the dielectric constant of the insulator and E_{BD} is the dielectric field strength at breakdown. As mentioned earlier in the ideal model, the phosphor is assumed to be insulating at voltages below threshold, and the sandwich

structure can be considered as three capacitors in series. Therefore, to emit electroluminescence without breakdown, the Q_{max} of the insulator has to be larger than the charge capacity of the phosphor at threshold voltage or above it. Table 2 lists the commonly used insulating materials in ac TFEL displays, such as Y_2O_3, Al_2O_3, Si_3N_4, Ta_2O_5, and a composite dielectric SiAlON.[39]

Electron-beam-deposited Y_2O_3[6] occasionally exhibits excellent dielectric properties, but it has been found to have poor reproducibility. Sputtered silicon nitride has been found to have high breakdown strength, but adhesion and film stress problems are associated with the use of pure sputtered Si_3N_4.[40] Aluminum oxide[39] can be deposited with good dielectric properties using reactive sputtering. Its advantages are moderately high dielectric constant of about 10 and excellent stability of display characteristics. However, it will react with the ITO layer and cause high dielectric loss. Tantalum oxide has a good dielectric constant of 25. It was found that the device employing Ta_2O_5 RF-sputtered films exhibited high brightness, low driving voltage, and high stability.[41] However, it too has a tendency to react with the ITO layer.

Single-material insulating films, as stated above, provide advantages of simplicity for fabrication. But for

Table 2. Physical properties of some common insulating materials used in AC TFEL devices.[31]

Materials	Dielectric Constant, ε_r	Breakdown Field, $E_{B.D}$ (MV/cm)	Charge Stroage Capacity ($\mu c/cm^2$)	Deposition Process	Remarks
Y_2O_3	12-14	1-3	1.2-3.2	E-Beam	Moisture sensitive, irreproducible
Al_2O_3	10-11	1-3	0.95-2.9	Sputtering	Reaction with ITO, poor efficiency
Si_3N_4	7	5	3.1	Sputtering	Poor adhesion, catastrophic breakdown
Ta_2O_5	25	2-3	4.4-6.5	Sputtering	Reaction with ITO
SiO	5	2.9	1.4	Evaporation	
SiAlON	8	8-9	5.6-6.4	Co-sputtering	Good barrier, less stress than Si_3N_4

practical manufacturing displays with high brightness and long life, extremely thin layers of excellent quality must be deposited with consistency. This difficulty has been found in single-material insulators. However, composite and stacked insulators allow the use of thicker layers in a compromise way, which are less sensitive to defects. The composite insulator, such as SiAlON, showed a brightness value of 1000 fL/Hz with a low dissipation and high charge storage capacity, well over 3 $\mu c/cm^2$.[39] In addition, SiAlON was also found to have less film stress problems than Si_3N_4. Stacked insulators, such as Al_2O_3:Ta_2O_5 system, are reported to yield an average dielectric constant between 10 and 23 to provide maximum protection for displays.[42] The properties and fabrication methods of some common insulating materials are compared and summarized in Table 2.

Recently, some thick ceramics have also been used as insulating layers as well as the substrate in thin-film electroluminescent devices to achieve low operating voltage and breakdown-failure-free operation.[43,44,45]

Generally speaking, optimum insulators can be obtained by selecting a proper dielectric constant and charge storge capacity. Silicon nitride, Si_3N_4, which has a moderate dielectric constant of 7, high charge storage capacity of 3.1 $\mu c/cm^2$ and high breakdown strength of 5 MV/cm, has been

thought to be the best dielectric. However, Si_3N_4 has adhesion problems with ZnS film.[39] Plasma-enhanced chemical vapor deposition (PECVD) silicon nitride layers have been used as the interlevel dielectric in multilevel metallization structure.[46] One of the important advantages of plasma deposited silicon nitride is its low intrinsic stress as compared to thermal CVD films. Therefore, PECVD silicon nitride dielectric layers are used in this project.

3. THIN FILM ELECTROLUMINESCENT FABRICATION TECHNIQUES

Thin film electroluminescent devices are thought to be excellent for flat panel displays because of the possibility of making large area and high field displays. Commercial large area, light emitting thin films, must be made very uniform with precise stoichiometry and desired crystallinity, low defect density, and stability over tens of thousands of hours. The stable, high field region must be so designed that there is no thermal runaway or local pinhole burnout. In ac TFEL devices, this is usually achieved by sandwiching the luminescent layer between insulating layers having high dielectric constants.

The stoichiometry of the zinc sulphide must be controlled because any variation in the stoichiometry leads to a change in the electrical properties. An increase in vacancies in the zinc sulphide will also affect the stability of the thin film. The grain size, the crystal orientation, and the nature of the crystalline boundaries of the zinc sulphide, all influence the characteristics of the display. It should be indicated that in a uniform transparent thin film, the high index of reflection of the zinc sulphide results in considerable total internal reflection. A rough surface will improve the light output.[47]

Only the preparation of the light emitting region will be considered in this chapter. ZnS:Mn is the main example. The TFEL devices can be made by a number of preparation technologies as stated in the following section.

Evaporation: The simplest method of depositing thin films makes use of heating a source material, ZnS:Mn, in a good vacuum system. In general, a deposition can be divided into three steps:

(1) vaporization and disassociation of the source material,

(2) transportation of material to the substrate,

(3) condensation of material on the substrate.

The last step is the most critical in obtaining a high-quality thin film. The major parameters are substrate cleanliness, substrate temperature, substrate angle and position with respect to the source, deposition rate, chamber pressure, and background gases. Although this method can produce uniform thin films, the stoichiometry, orientation and crystallinity of the zinc sulphide cannot meet the requirements for TFEL devices.[48] Addtionally, the preparation of ZnS thin films by electron-beam evaporation also has shown that the grain size and shape change with distance from the substrate.[49]

The complex effects of impurities and annealing treatments on the properties of the zinc sulphide films have

also been reported.[50,51] In most cases, the zinc sulphide films were annealed after evaporation. These studies verified that there are considerable variations between the source material and the deposited film. Also, impurities, especially chloride, affect the nature of crystallite size of the ZnS films, as well as the cubic-hexagonal ratio of the ZnS lattice. Furthermore, there is much evidence of the interaction of the various insulating layers with the ZnS. Some of this interaction can be avoided by the introduction of buffer layers such as CaS[52] between the ZnS and the insulating layers.

Atomic Layer Epitaxy (ALE): The development of atomic layer epitaxy and its application in manufacturing high quality TFEL devices was first contributed by Suntola.[53] The process of ALE is carried out by separate surface reactions between the surface to be grown and each of the components of the compound serving as reactants. Zn or a Zn compound and S or H_2S are the reactants in this case. The temperature of the surface is kept high enough to prevent the condensation of each reactant. ZnS layers are deposited by interaction, resulting in a self-controlled growth of one atomic layer at a time. However, this process is extremely time-consuming. The crystallinity of ZnS thin films produced by this method are good because of its polycrystalline

structure. ALE has been used in the preparation of flat panel displays and to large information boards and a module with 2880 characters has been described.[54]

Sputtering: In the sputtering process, the ZnS thin films can be deposited directly from the target to the substrate in a gas plasma at low pressure. The atoms or molecules are ejected by the bombardment of inert gas ions of sufficient energy. Because the target materials are insulating, radio frequency (rf) voltage is usually required. The rf sputtered ZnS:Mn TFEL devices have been shown to have better performance than evaporated films.[55] Sputtering appears attractive as a good industrial process for the preparation of ZnS:Mn. Indeed, it is employed for the deposition of the ITO films and many insulating layers used in the TFEL device. The main problem with this technique is that it is difficult to control film uniformity and crystallinity. Small variations in thickness of ZnS film will have major effects on the field distribution, and can be seen with a lack of uniformity in the light emitting region. Although good results on rf sputtered thin films using ZnS target have been achieved, the difficulty in producing large areas has not been overcome.

Chemical Vapor Deposition (CVD): Chemical vapor deposition was one of the earliest techniques to be developed

for the preparation of TFEL devices. The earlier techniques used the vapor reaction of zinc chloride with hydrogen sulphide to prepare zinc sulphide thin films. However, the residual halide, together with the non-uniform films, led to rapid burnout or to catastrophic breakdown.[56] The life of the ZnS films was very short. Not until the development of metal-organic chemical vapor deposition (MOCVD), were these problems solved. The development of MOCVD techniques, which have been successfully and widely used for the deposition of ultra pure epitaxial layers of many III-V and II-VI compounds of interest in the semiconductor industry, has led to a revaluation of their application for ac TFEL preparation.[57,58,59,60]

The potential advantages of MOCVD techniques are better stoichiometry, more uniform doping and crystallinity control. Another advantage is that MOCVD is a low temperature deposition treatment. This technique produced the ac TFEL displays with a fairly high brightness of 9300 cd/m2[61] and can be employed for large-area TFEL devices, 1000 x 1000 mm^2[62], for example. In addition, the MOCVD technique is advantageous in the inexpensive preparation of large-area thin films. This technique can be divided into two categories: decomposition and additive MOCVD.

Decomposition MOCVD: Metal-organic chelate compounds,

such as zinc dialkyl dithiocarbamate

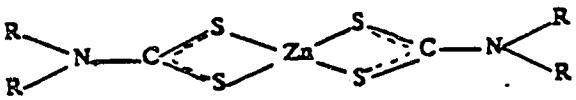

and zinc xanthate,

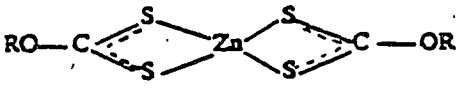

are usually used to deposit ZnS.[63] These compounds contain zinc and sulphur as source materials are easy to decompose at a raised-temperature substrate. For example, under atmospheric pressure conditions, with a N_2 carrier gas, the source material, zinc diethyl dithiocarbamate, is heated to temperature in the range 190°C-250°C and vapor is carried to the heated substrate (380°C-450°C), where the reaction occurs.

$$[(C_2H_5)_2NCS_2]_2\,Zn \xrightarrow[N_2]{400^{\circ}C} ZnS + [(C_2H_5)_2NCS]_2S \qquad (20)$$

Additive MOCVD: It has been shown that thin film single crystal layers of ZnS can be grown on to a variety of substrates by direct reaction at atmospheric pressure, of dimethyl zinc and hydrogen sulphide, using hydrogen as the carrier gas.[57] Generally, the fabrication of the light emitting region, ZnS:Mn, in TFEL devices using additive MOCVD

technique can be described as follows. A substrate is usually heated to the desired temperature between 300°C-400°C. Dimethyl zinc (DMZ) $Zn(CH_3)_2$ and hydrogen sulphide H_2S, which pass over the substrate by a carrier gas, decompose when heated by the substrate to form a ZnS thin film. The basic reaction to produce ZnS is

$$Zn(CH_3)_{2(g)} + H_2S_{(g)} \rightarrow ZnS_{(s)} + 2CH_{4(g)} \qquad (21)$$

Then, the luminescent centers Mn can be introduced into the system either by doping with a volatile Mn compound, such as TCM[57,64] (tricarbonylmethyl cyclopentadienyl manganese) during the film growth, or by subsequent thermal diffusion into MOCVD-prepared ZnS film.[59] Using dimethyl zinc and H_2S as source gases and TCM as the dopant gas, Hirabuyashi and Kozanaguchi[65] developed very high luminance ZnS:Mn electroluminescent devices, more than 5000 cd/m^2 operated at 5 kHz and 130 V. However, this technique showed that TCM was disadvantageous because a substrate temperature above 450 °C is necessary to achieve efficient doping, and because a high substrate temperature causes the ZnS film and indium tin oxide (ITO) to react.

To avoid the above disadvantages, thermal diffusion of Mn into MOCVD-prepared ZnS film is used. The ZnS:Mn film is typically annealed at 400 °C for one hour at a high vacuum

condition (10^{-6} torr). It was found that ZnS:Mn EL devices fabricated by this method exhibited high brightness and efficiency.[59] In addition, these devices showed highly stable operation and high breakdown voltage. Therefore, this method will be employed in this work. The detailed fabrication sequence of ZnS:Mn EL devices and the schematic diagram of the MOCVD system used in this work will be presented in the following chapter.

4. EXPERIMENTAL PROCEDURES

4.1. Reactor Modification of the Metal-Organic Chemical Vapor Deposition (MOCVD) System

The existing geometry of the MOCVD reaction chamber used in previous work resulted in a thickness uniformity of ZnS film which was very poor.[1] The thickness was radiatively distributed from the deposition center and almost no ZnS deposited at the edge of substrate glass. To improve the thickness uniformity of ZnS film, a modification of the reactor was made. As suggested by Dr. Burt Masters of SJSU, a shower head was incorporated at the end of the dimethyl zinc inlet nozzle. The purpose is to more uniformly introduce the reactant gas to the glass substrate by distribution through some small holes. In order to achieve this purpose, the total area on the bottom of this shower head was designed to cover the entire glass substrate. We, therefore, hoped to obtain good thickness uniformity of ZnS film. Figure 7 shows the dimension of this shower head, and in Appendix section, Figure 24 also shows the assembly drawings. The material used for the shower head was 0.05 mm thick stainless steel sheet. The results of this design improvement will be discussed in Section 5.1, below.

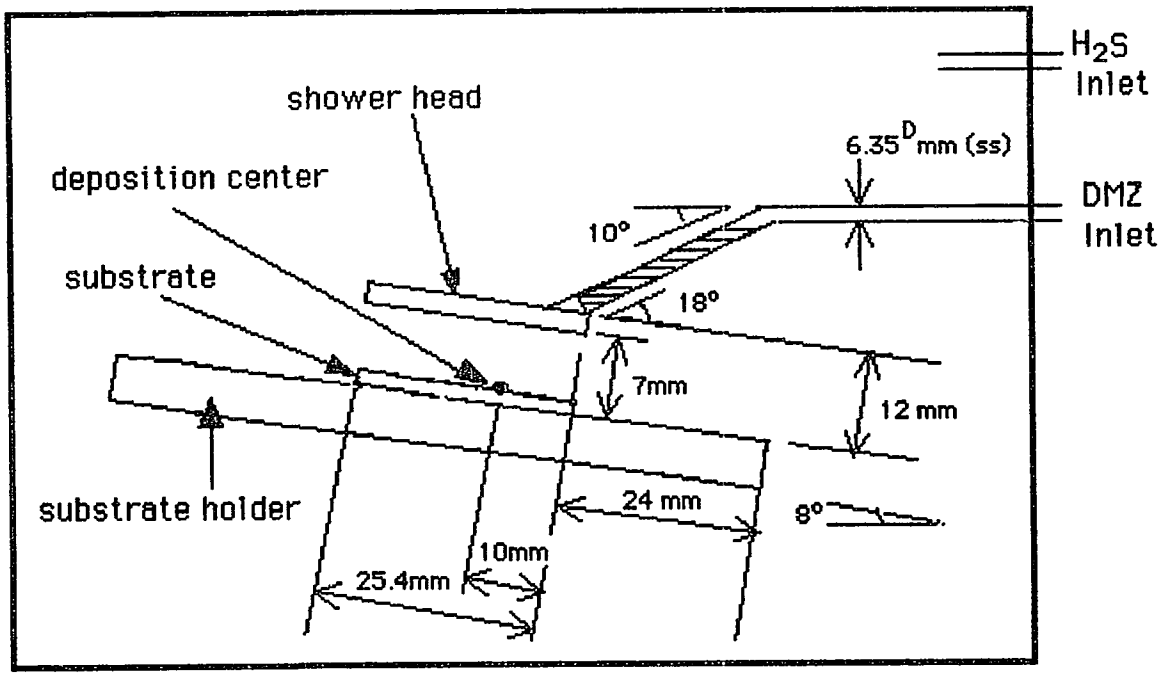

Figure 7. Reaction chamber geometry of MOCVD system used in this project and the relative position of each component. The whole MOCVD system is also shown in Figure 9.

4.2.Device Fabrication

The entire fabrication process of this TFEL device is shown in Figure 8. Three-inch long and one-inch wide glass coated with 1000Å transparent indium tin oxide (ITO) film, purchased from Hoya Corporation, was used as the substrate. The substrate was cleaned with boiling acetone and methanol solvents three times before deposition. First of all, a silicon nitride film about 2215Å thick with a refractive index of 2.035 was deposited onto the ITO glass by the plasma-enhanced chemical vapor deposition (PECVD) method as shown in Figure 8 (b). The PECVD machine (Semigroup) was provided by the Integrated Circuits Laboratory at Stanford University. Silicon nitride was chemically deposited by reacting silane (30 sccm) and ammonia (200 sccm) in a nitrogen discharge at temperature of 214 °C and pressure of 2.0 torr. Subsequently, to expose the ITO electrode, plasma etching (CF_4 + O_2), Figure 8 (d), was used after spreading photoresist on top of the silicon nitride layer by cotton swabs, as shown from Figure 8 (c) to (f).

The ZnS:Mn phosphor layer was then prepared by additive MOCVD ZnS, Figure 8 (g), and doped with Mn, Figure 8 (h). The MOCVD reactor at San Jose State University was built and modified by Marc Jensen[66] and Hoa Do[67], respectively. The schematic diagram of the MOCVD reactor is shown in Figure

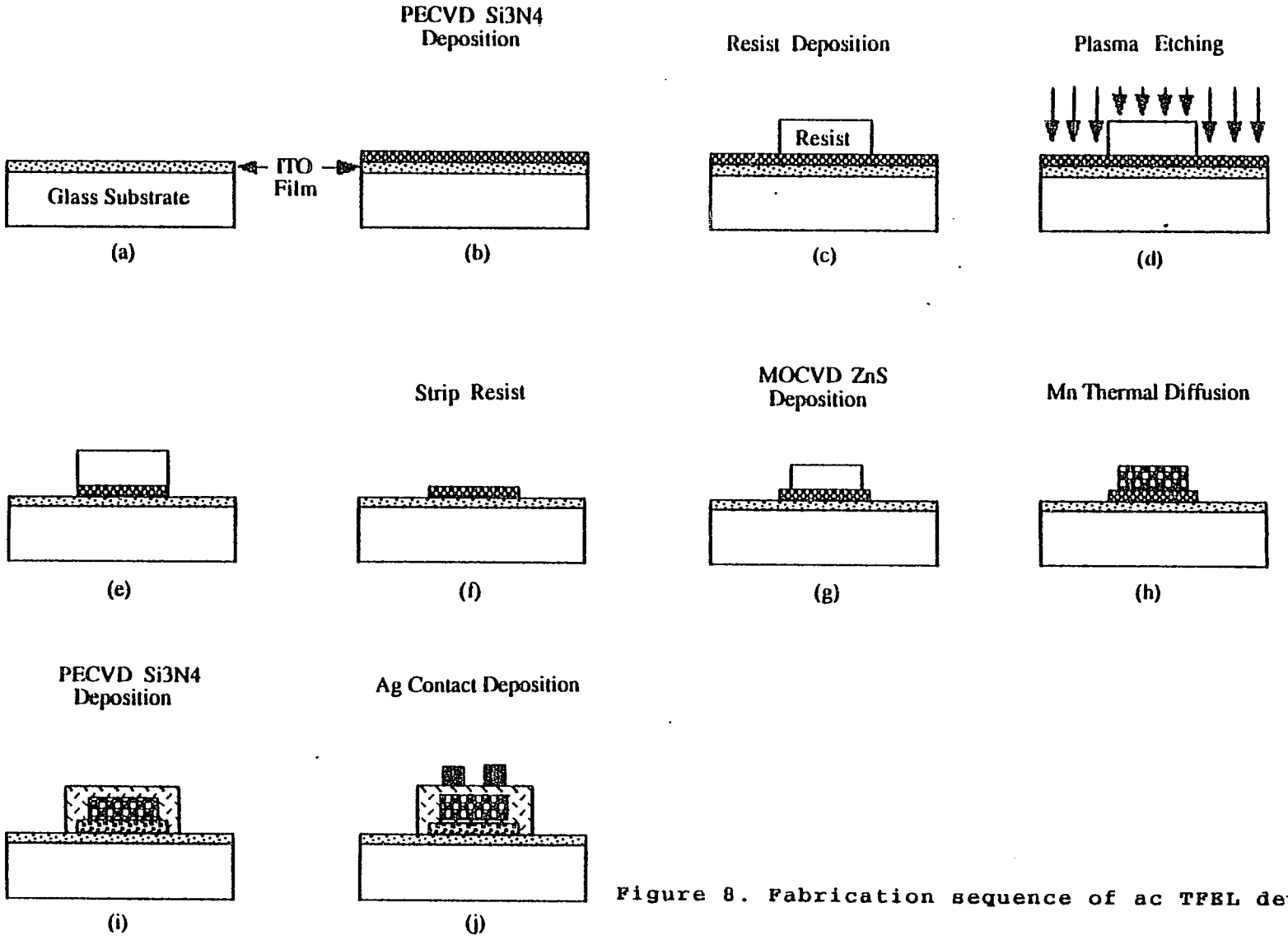

Figure 8. Fabrication sequence of ac TFEL devices.

9. Ten percent hydrogen sulphide (H_2S) and 1% dimethyl zinc (DMZ) in helium were used as reactants to deposit the ZnS. Deposition was conducted at a pressure of about 6 to 7 torr and a temperature of 300 °C. The basic reaction used to produce ZnS is

$$(CH_3)_2Zn_{(g)} + H_2S_{(g)} \rightarrow ZnS_{(s)} + 2\ CH_4{}_{(g)} \qquad (21)$$

The flow rates of DMZ and H_2S were controlled at 15 sccm for DMZ and 60 sccm for H_2S, respectively.

The introduction of Mn into ZnS was carried out by thermal diffusion. This process can be divided into two steps: pre-deposition of Mn on ZnS and drive-in. After the deposition of ZnS film, about 0.5 weight percent of Mn dopant was evaporated onto the ZnS using vacuum evaporation under a pressure of 10^{-3} torr. The Mn source was placed in a tantalum boat, and the distance between the source and boat was 18 cm. Thus, the accurate quantity and thickness uniformity of Mn could be well controlled by using the small-area source equation.[68] The detailed calculation and discussion is referred to the Reference 54. After Mn deposition, the substrate was quickly moved to a high vacuum chamber in which drive-in of Mn into the ZnS film proceeded. The MOCVD vacuum chamber was selected to serve this purpose. In order to effectively diffuse Mn and eliminate particles during thermal

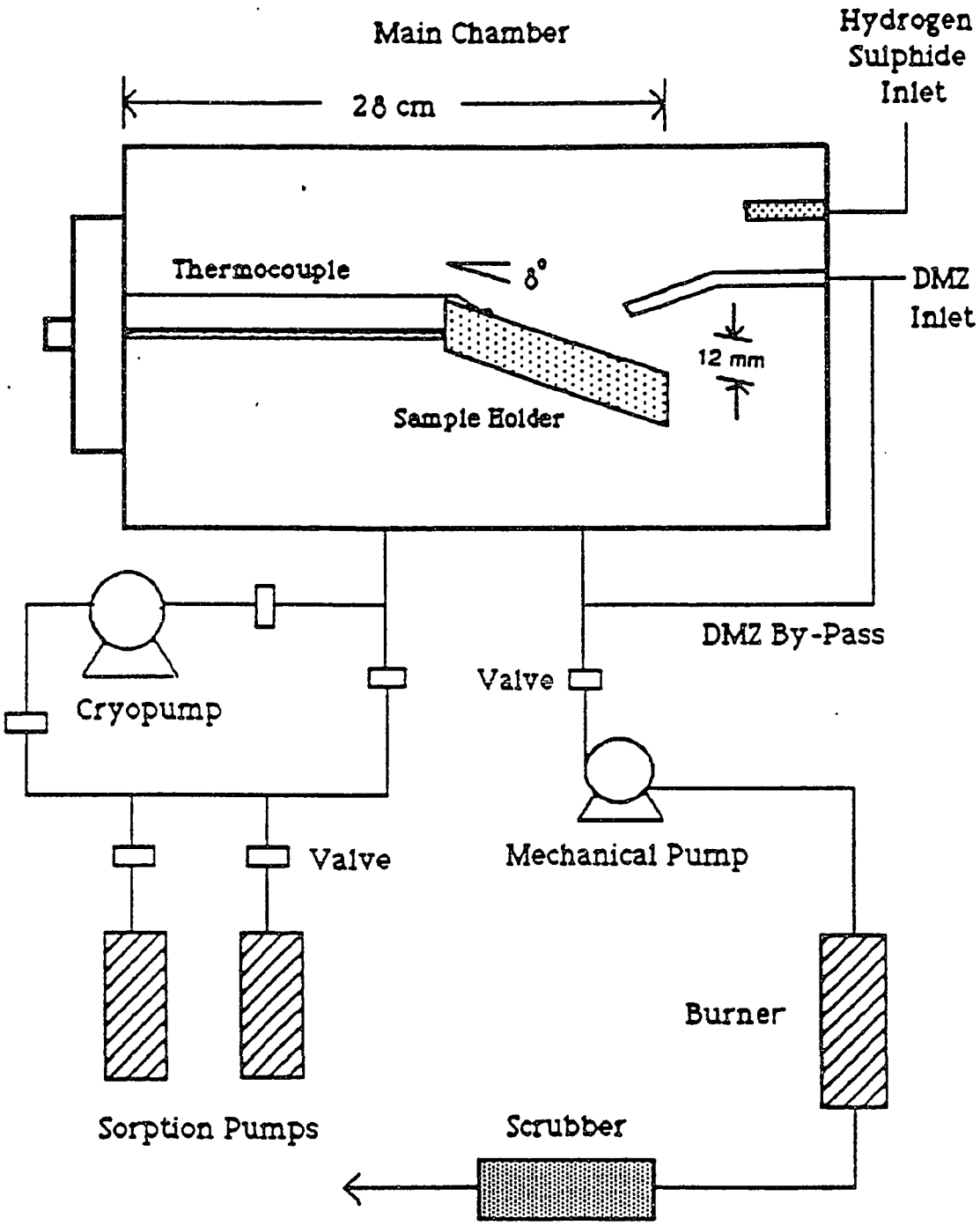

Figure 9. Schematic diagram of the MOCVD system employed in this work.[1]

diffusion, the process was carried out at a temperature of 400°C and a pressure of about $1x10^{-7}$ torr for an hour. The high vacuum was achieved by using two sorption pumps and a cryopump.

After the deposition of ZnS:Mn, a secondary PECVD Si_3N_4 insulating layer was deposited onto the ZnS:Mn layer by the same method mentioned earlier as shown in Figure 8 (i) . The second Si_3N_4 layer has thickness about 2520Å and a 2.036 index of refraction. Finally, silver electrical contacts were made by vacuum evaporation on top of the Si_3N_4 layer. A piece of paper was used for masks to make the contacts. Several aluminum electrical contacts were also made by a different evaporator which is located in the IC lab at SJSU. Approximately, a single substrate could make 16 devices. The entire light emitting area of a device was about 9 mm^2 (3mm x 3mm). The completed thin-film electroluminescent device is shown in Figure 8 (j).

4.3.Device Characterization

The device fabricated by the above steps emitted yellow light when an alternating voltage was applied between the ITO and the Ag electrodes. The whole test set-up is shown in Figure 10, and is similar to that employed in Chuang's thesis study.[1] First, the sinusoidal voltage, used to produced a

reversed voltage polarity, was generated from a function generator (HP 3310A) with desired frequency, 1 kHz, and then was amplified through a high power amplifier (Trek 70/750). This generated power, from 27 volts to 400 volts, was sent to the ITO and Ag electrodes of the device. The brightness was measured with a photomultiplier tube (AMPEREX XP 21028) under 1 kHz sine-wave voltage excitation. During the measurements, both the device and photomultiplier tube were placed into a light-tight plastic container to prevent the interference from ambient light. The photomultiplier tube was set at high gain voltage of 1200 volts. The device sat in front of the photomultiplier tube at a distance of about 3 cm. The measured brightness signal was separated into two channels; one was sent to a oscilloscope and the other one was sent to a X-Y recorder. Thus, the phase relationship between the generated electroluminescence and applied voltage, and the data of relative brightness of luminance versus frequency, current and output applied voltage could be directly obtained and studied.

Also, an attempt was made to record the emission spectrum of electroluminescence. This was done by using the photomultiplier and a monochromator (BAUSCH & LOMB) to measure the relationship of the EL intensity and wavelength.

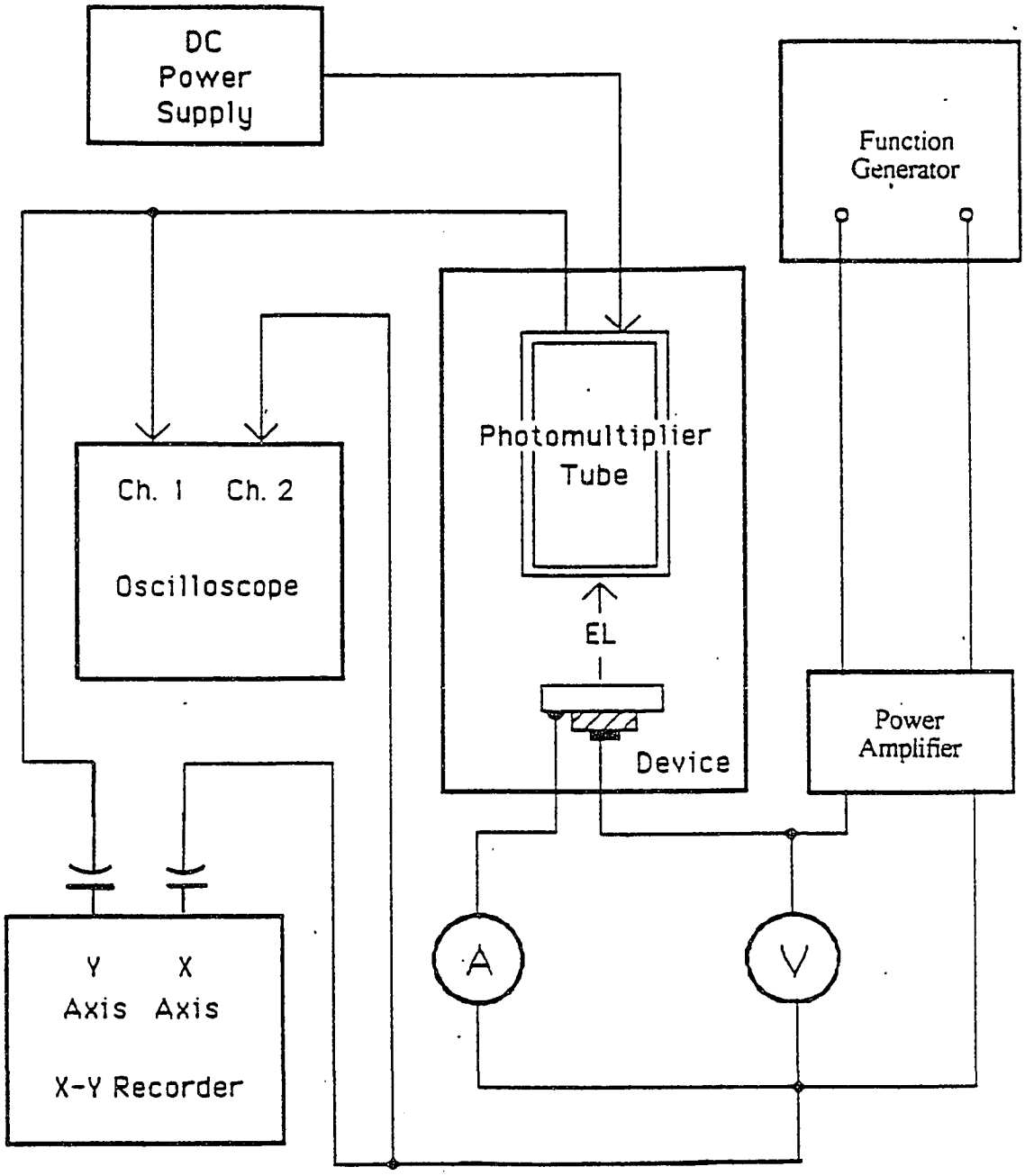

Figure 10. Schematic diagram of the experimental set-up for measuring and recording relative brightness, voltage, and current.[1]

5. RESULTS AND DISCUSSION:

5.1.Uniformity and Characterization of ZnS Film

Before incorporating the shower head at the end of dimethyl zinc inlet nozzle, the thickness of ZnS film was radiatively distributed from the deposition center and nearly no ZnS deposition at the edge of substrate glass. This situation could be easily seen with bare eyes. The maximum thickness variation from the edge to deposition center was about 87%.[1] After the shower head installation, the entire deposition area (25.4 mm x 25.4 mm) was deposited with a more uniform ZnS film as will next be shown.

Figure 11 shows the thickness measurements by profilometry on a ZnS film deposited substrate after the shower head installation. Here, the thickness uniformity, U, is determined by the right-edge point, X1, for example, and the correspondent point on the left edge, Y1. The uniformity is around 25%. This value is defined as follows,

$$\text{Thickness uniformity } U = \frac{|X1 - Y1|}{Y1} \times 100\% \quad (22)$$

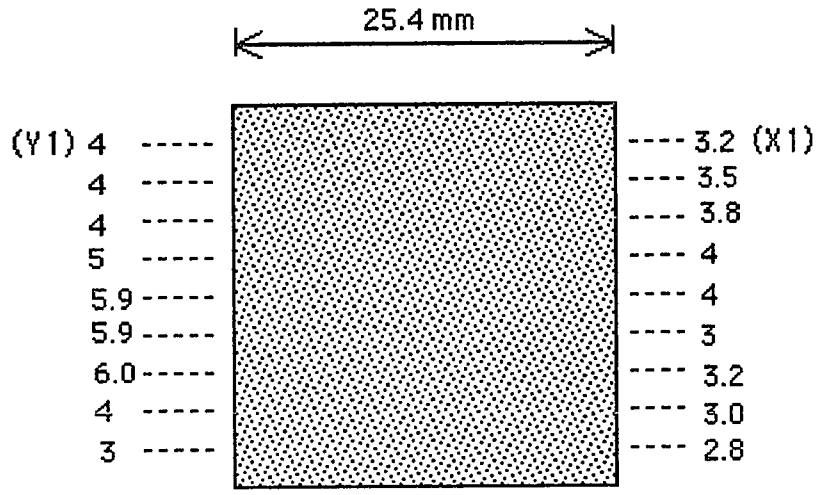

Figure 11. Thickness distribution of ZnS film after the shower installation. The thickness value is in a unit of 10^{-4} cm.

The whole uniformity is within 49%. Unfortunately, we did not measure the thickness in the central region in order to compare our results with the previous thickness profile on the ZnS film. However, the entire deposition area now can be deposited with a more uniform and less varied thickness of ZnS film.

The ZnS films were characterized by X-ray diffractometer (XRD) and Scanning Electron Microscope (SEM). Figure 12 shows the XRD pattern of the ZnS film prepared by MOCVD at 300 °C. The examined ZnS film was deposited on a glass substrate with a thickness of 4 μm. The wavelength of the X-ray was 0.15 nm. The diffraction angle, 2θ, and the intensity of the diffraction beam were automatically plotted by a chart recorder. The XRD pattern shows a major peak at the diffraction angle of 28.6°. This peak is compared with the standard XRD pattern for ZnS, in order to determine the crystal structure.[69] The result shows a cubic polycrystalline structure with a preferred (111) orientation.

Figure 13 is the SEM micrograph of the surface of the same ZnS film. The surface of the MOCVD-prepared ZnS film is polycrystalline, consisting of grains with diameters of about 1.5 μm.

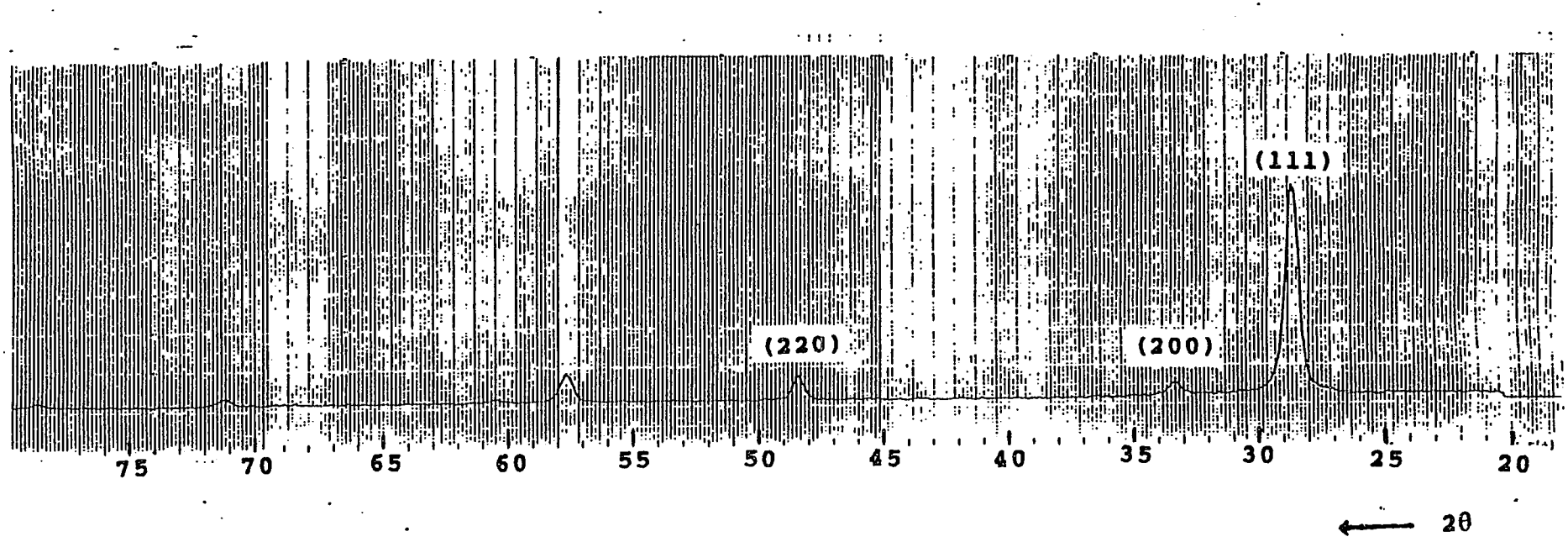

Figure 12. X-Ray diffraction pattern of ZnS film prepared by MOCVD.

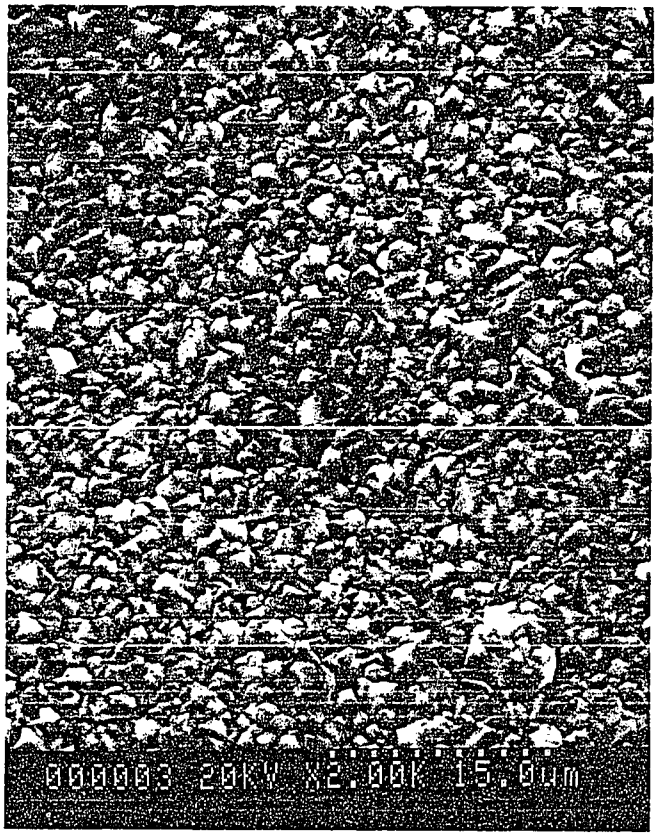

Figure 13. SEM micrograph of MOCVD-prepared ZnS film surface.

5.2. Brightness-Voltage (B-V) and Current-Voltage (I-V) Characteristics

Figure 14 and 15 show B-V characteristics for the ac TFEL devices. In Figure 14, the B-V characteristic includes two threshold behaviors. For device C4, the brightness increases dramatically when the applied voltage exceeds 100 volts and forms a peak. This applied voltage is defined as sub-threshold voltage and will be explained in the next section. Then, the brightness decreases to the applied voltage around 210 volts where the brightness reaches a constant. After that point, the normal B-V curve is exhibited. The normal B-V curve will be only considered in this section.

As seen in Figure 15, the brightness increases dramatically as applied voltage exceeds the threshold voltage, V_{t1}, for example, 220 volts for device C4, and then tends to saturate at high voltage regions. Here, the threshold voltage is defined as the voltage at which noticeable light emission begins. This value can also be determined from I-V characteristic in Figure 16. As seen in Figure 16, the current passing through the device increases linearly as the applied voltage increases. The slope of the I-V changes at the point where the avalanche current occurs. This point defines the threshold voltage.

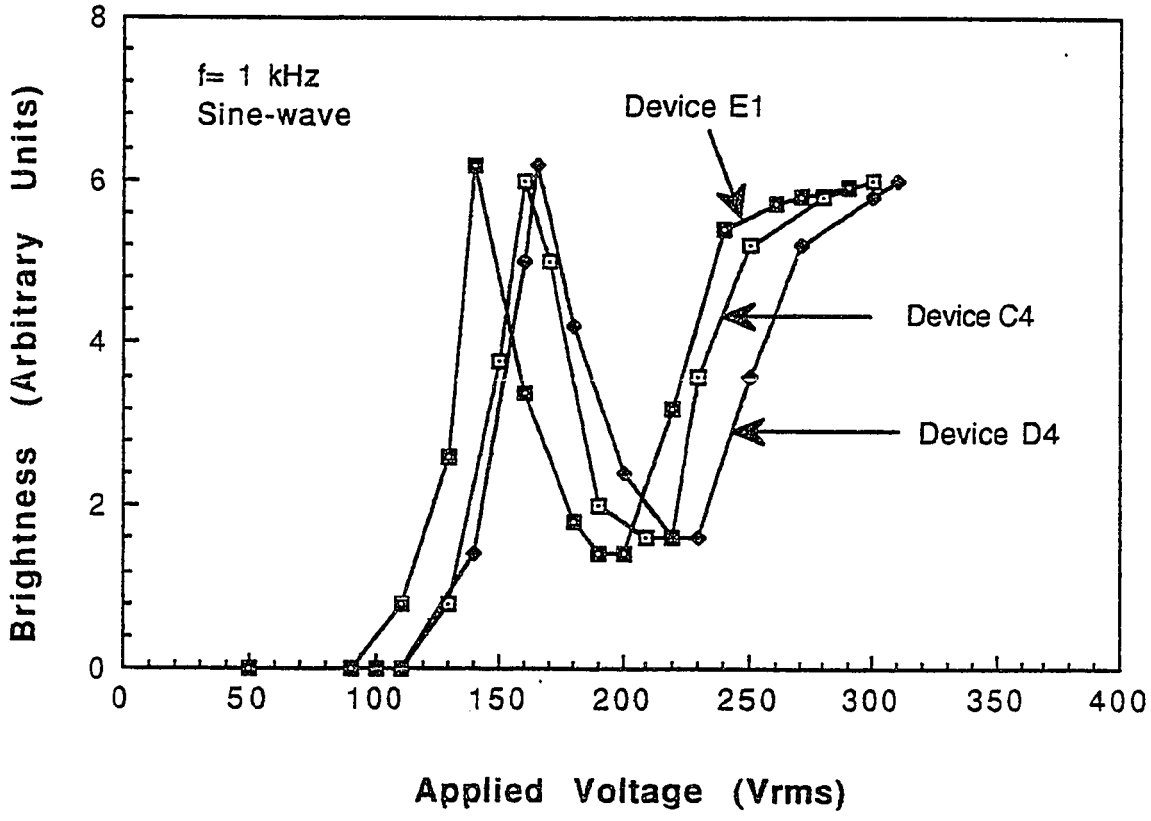

Figure 14. Brightness vs voltage characteristic of ZnS:Mn TFEL devices using Si_3N_4 insulator operated with 1 kHz sine-wave voltage. (Note: an rms voltage of 100 volts corresponds to peak-to-peak excursions of +140 volts to -140 volts.)

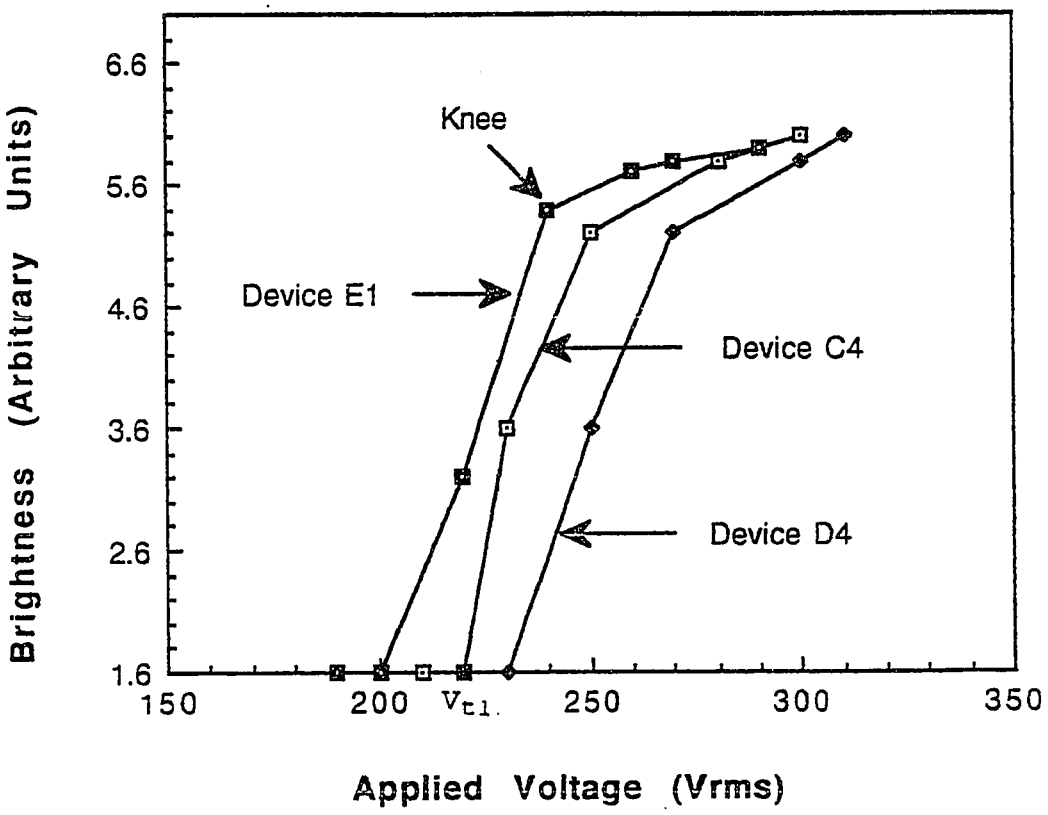

Figure 15. Normal brightness-voltage characteristics of ZnS:Mn TFEL devices under 1 kHz sinusoidal power.

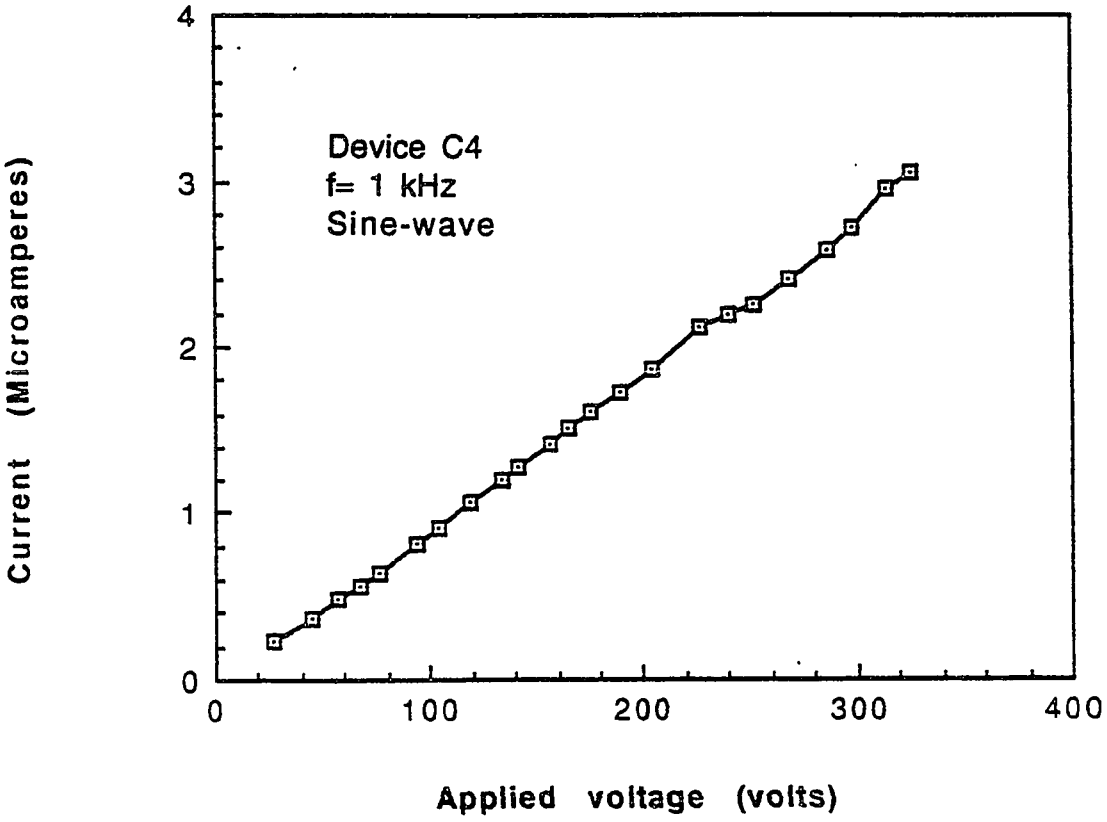

Figure 16. Typical current-voltage characteristics of ZnS:Mn TFEL devices under 1 kHz sine-wave.

As shown in Figure 15, device C4, D4, and E1 all exhibit very similar B-V characteristics, though they were fabricated on different substrates with separate fabrication processes. In other words, that means that the performance reproducibility of these TFEL devices is good. A very steep B-V characteristic was observed. This was thought to be due to the trapping and tunneling of electrons from deep levels.[70] This phenomenon was observed in all functioning devices. An unique point on B-V curve is the knee as pointed out in Figure 15. The brightness at the knee of the B-V curve is very important. The knee of the B-V curve is approximately the optimum luminous efficiency and the nominal operating point.

The threshold voltage was found to be in the range of 200 to 285 rms volts. These values are a little bit higher than Chuang's, 100 to 220 rms volts. But most of them are concentrated between 200 to 250 rms volts as referred to Table 3. Our devices seemed to exhibit more steady B-V characteristics than Chuang's. However, the short operating lifetime has been playing a key "killer effect" on our devices. Low field breakdown, below 200 volts, was frequently found on substrate D and E. The longest operating lifetime was found to be 3 hours on device C5. The average lifetime reported by Chuang was about two to three hours. Removing the water content from the TFEL devices was attempted by baking

the devices in a vacuum for 24 hours. The results showed that the devices on substrate D and E exhibited very short lifetime of about few seconds, though the B-V and I-V characteristics were still seen. The variations of lifetime on substrate C, D, and E have remained unexplained, even though the processing steps of each device is well controlled. Presumably, the Mn concentration on each device has a different distribution. Since we did not precisely measure the Mn concentration for each device, the device could have different dopant concentrations than that calculated from the small-area source equation.[54] In addition, the impurity level in the evaporator could also play a key effect on the low field breakdown situation. All these reasons could cause the problem of the short lifetime found on our devices. Currently, commercialized ac TFEL devices have typical operating lifetimes of over 10^4 hours. The investigation of device breakdown will be presented in detail later on. The device information and testing results are summarized in Table 3.

Table 3. Device Histories and Testing Results

Substrate	Device	First Si_3N_4 (Å)	ZnS (Å)	Second Si_3N_4 (Å)	Mn wt%	Threshold Voltage (volts)	Breakdown Voltage (volts)	Operating Lifetime
C	1	2215	9000	2520	0.5	285	354	10 minutes
	2	"	8000	"	0.56	NA	395	40 minutes
	3	"	9000	"	0.5	246	390	2 hours
	4	"	8000	"	0.5	220	328	2 hours
	5	"	7000	"	0.64	210	330	3 hours
*D	1	"	8000	"	0.5	NA	200	Few seconds
	2	"	6000	"	0.67	245	290	Few seconds
	3	"	8000	"	0.5	NA	260	Few seconds
	4	"	8000	"	0.5	230	310	Few Seconds
E	1	"	8000	"	0.5	200	290	2 minutes
	2	"	8000	"	0.5	NA	190	Few seconds
	3	"	5000	"	0.8	NA	148	Few seconds
	4	"	5000	"	0.8	NA	100	Few seconds
	5	"	8000	"	0.5	NA	120	Few seconds
	6	"	5000	"	0.8	246	350	5 minutes

* Substrate was baked to remove moisture at 140 °C for 24 hours in vacuum condition, 28 inHg, after the devices were made.

5.3.Sub-threshold Emission B-V Characteristics

An interesting phenomenon in the B-V characteristic of our TFEL devices was observed. Unlike the normal part of B-V curve shown in Figure 15, Figure 17 shows that a large peak emerges before the device exhibits the normal B-V characteristic. This peak starts as the applied voltage is 100 volts, then the brightness increases as the applied voltage rises and reaches a maximum value at 160 volts. After that, the B-V curve decreases to a low brightness region. This sub-threshold emission is rarely seen in TFEL devices. We thought that this light emission might be due to the excitation from some impurities existing in the devices. Therefore, we tried to measure the emission spectrum by setting a monochromator to record this light emission spectrum at the maximum brightness region. Unfortunately, no emission spectrum was obtained for our devices. However, we were able to measure the light emission spectrum from a yellow light-emitting diode (LED). Perhaps the reason why we could not get any light emission spectrum was due to the weak intensity of the light source and insensitivity of the measuring equipment. Since we have run out of the devices, this attempt has to be surrendered. In future work, the successor can try to use other more light sensitive equipment to achieve this task.

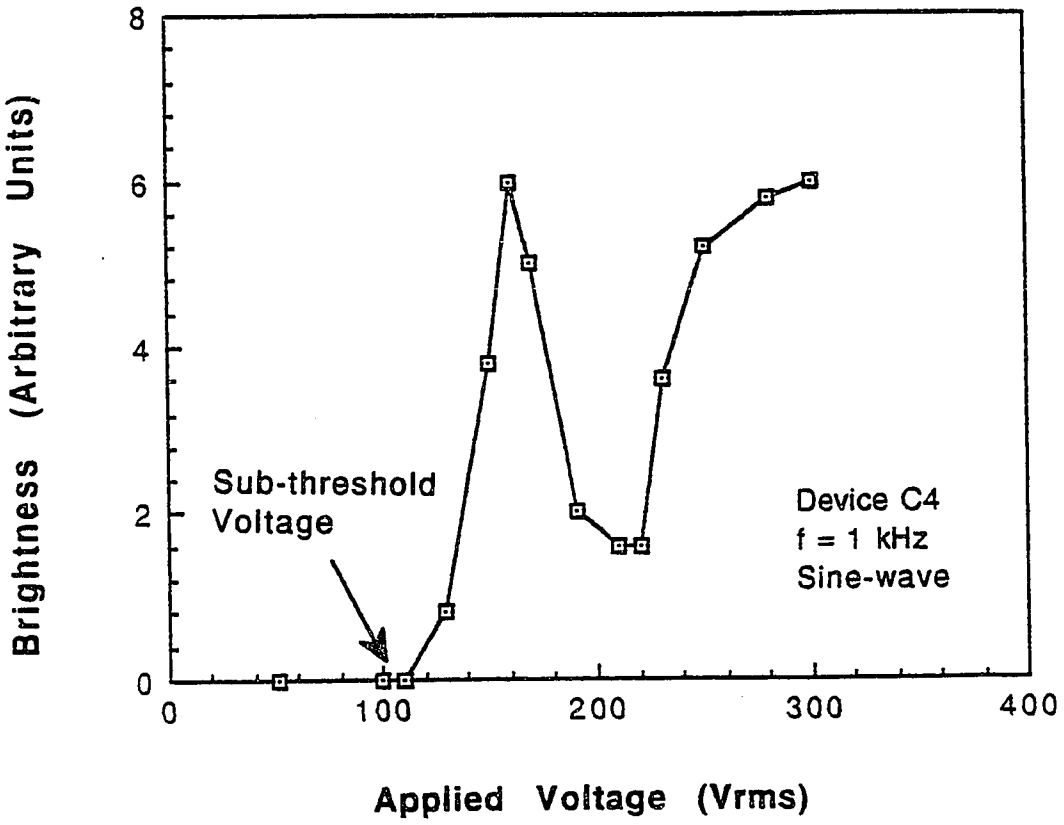

Figure 17. Subthreshold emission of B-V characteristic from C4 TFEL device under 1 kHz sinusoidal power.

5.4.Aging Characteristics

It is well known that the threshold voltage for TFEL devices increases with operating time and then gradually becomes constant.[6] Figure 18 shows the shifting of the threshold voltage, from 200 to 230 rms volts, on operating time for the TFEL device C5 during operation for 3 hours under 1 kHz sine-wave voltage excitation. The measurement was done in the following steps. The initial B-V characteristic was first measured, then the applied voltage was decreased to a fixed value below threshold value, 27 volts in this case, and the applied voltage was kept there for three hours. After three-hour aging, another B-V characteristic was measured again.

As shown in Figure 18, the brightness versus applied voltage characteristic shifts toward the higher voltage side as time elapses, but the saturation brightness does not change. This threshold voltage movement in the brightness-voltage characteristics with operating time is called aging effect. This aging effect in TFEL devices was thought to be due to the formation of deep traps in bulk ZnS and the interface between the ZnS and the insulators, which lead to a higher threshold voltage being required to initiate electron tunneling.[71] The formation of deep traps may be

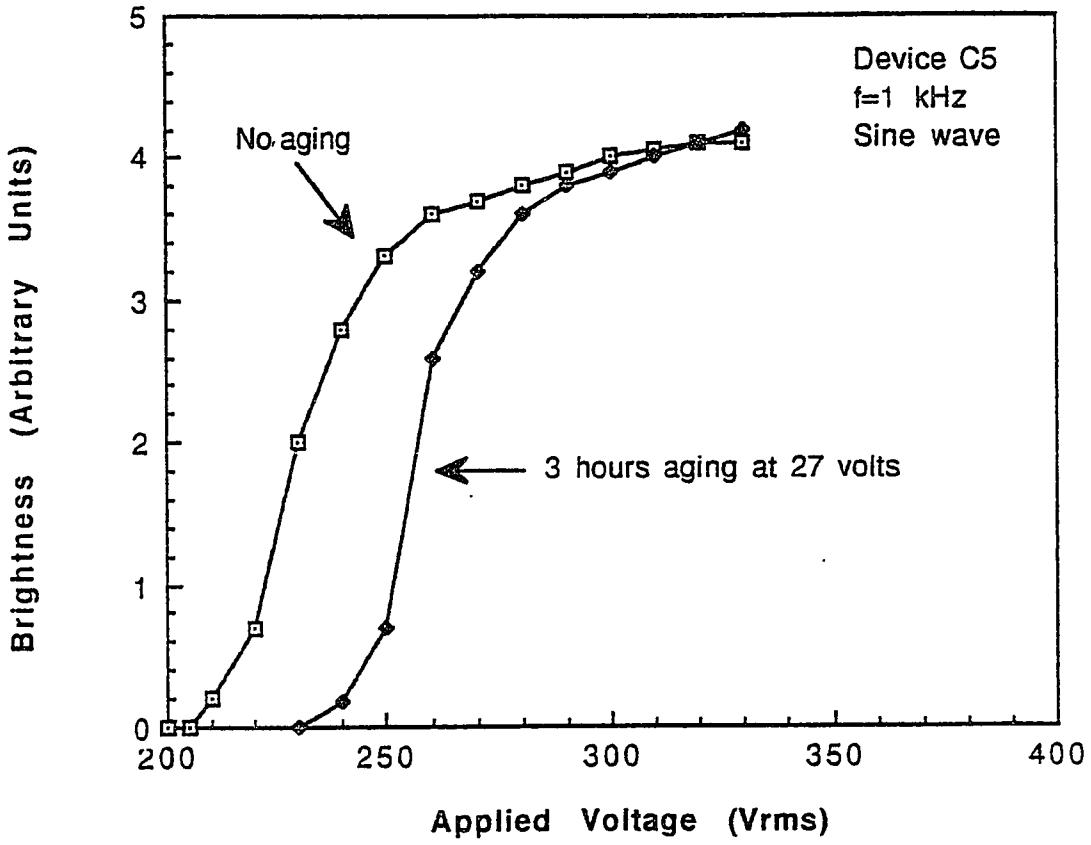

Figure 18. Brightness vs voltage characteristics for an aged device. The device was aged at 27 volts using 1 kHz sine-wave excitation.

due to the diffusion of atoms in the crystal, or chemical reactions under the influence of the electrical field. Although our devices did not have a long enough lifetime to obtain more convincing data, this phenomenon was observed for most of the working devices. Aging is a very important factor to the design of displays. If these initial stabilization effects are significant, the panel must be pre-conditioned before installation or the panel may show image ghosting.

5.5.Memory Effect

One of the B-V characteristics observed in the present ac TFEL devices is the so-called memory effect, as shown in Figure 19. When a sinusoidal voltage with frequency maintained at 1 kHz was applied to the device and slowly increased to the value close to breakdown, 320 volts in this case, a normal B-V curve was obtained. If the frequency was still unchanged and the voltage was decreased from 320 volts, a different path is followed. This loop is a so-called hysteretic loop, and this phenomenon is known as the memory effect.

This effect refers to a multilevel light output stability at the same applied voltage amplitude. The memory effect is believed to be due to the storage of space charge at the ZnS-insulator interface regions during power

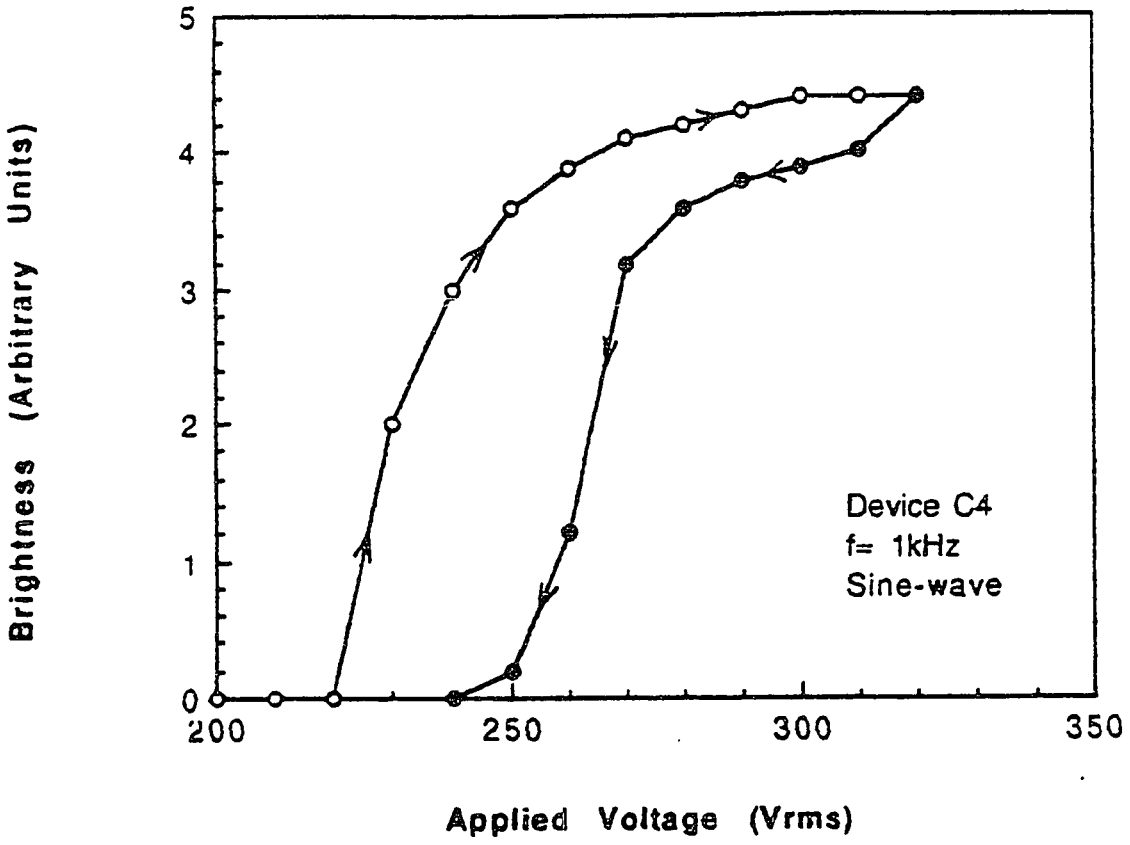

Figure 19. Hysteretic B-V characteristic for an ac TFEL device using Si_3N_4 insulators under 1 kHz sine-wave voltage.

application, thus forming an internal field which adds to the external field on voltage reversal, when the device is driven by alternating current, resulting in enhanced light emission.[35,36] This effect should result in the curve shifting toward lower applied voltage region. However, in our devices the curve shifted toward higher applied voltage. To explain this phenomenon obtained in our devices the charge stored at the ZnS-insulator interface has to be investigated. Possibly, it was due to chemical reactions occurring between PECVD silicon nitride and ZnS interface under high electric field (about 10^6 V/cm), resulting in a chemistry and morphology change in the interface and causing this behavior.

5.6.Lifetime Optimization Brightness-Time (B-T) Determination

Figure 20 shows brightness vs operating time for TFEL device operated at constant voltage in a typical saturation region of B-V characteristics. In the Si_3N_4 double insulated device, the brightness decreases gradually with operating time. The degradation of brightness is considered to be due to metal electrode peeling caused by impurities or moisture. More detailed discussion will be presented in next section.

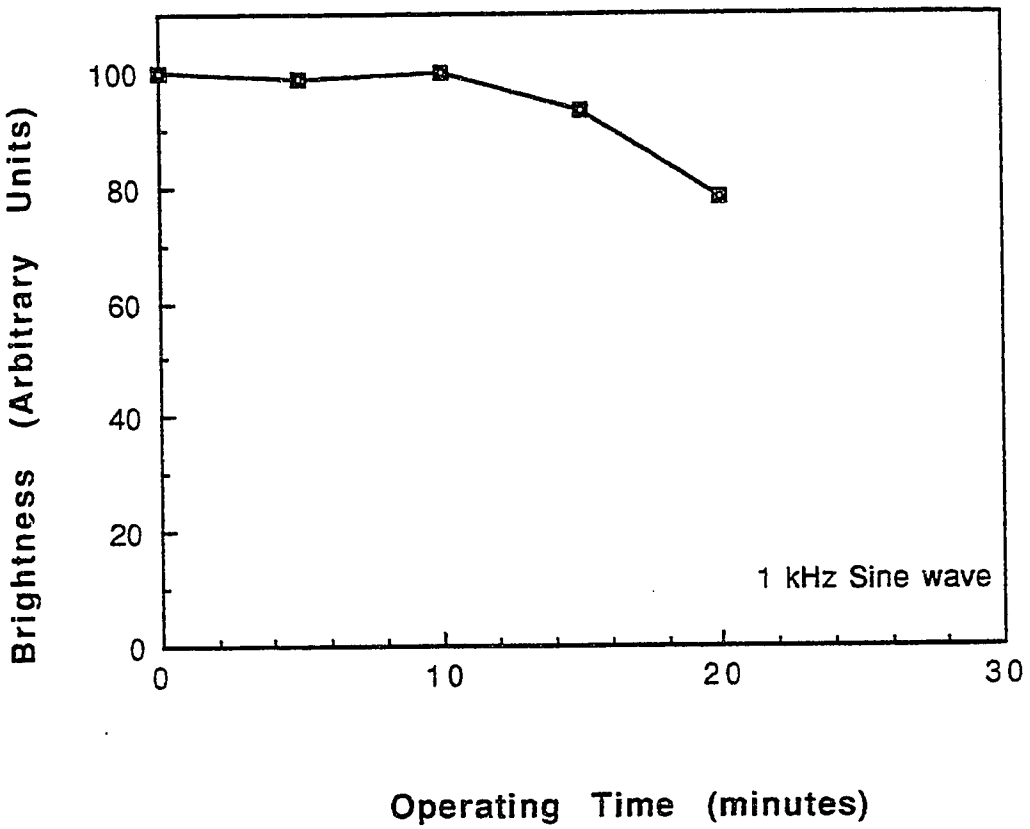

Figure 20. Brightness vs operating time for a TFEL device operated at a constant voltage.

5.7.Degradation Mechanisms

The most serious problem found on the TFEL device performance is the short operating lifetime that the devices exhibit through most devices' tests. The longest operating lifetime was found to be about 3 hours, as noted in Table 3. Most of the device failure occurred within the first few minutes of operation. Low-field breakdown at the voltage below 200 volts was often observed during the operation of the TFEL devices. Blue electrical arcs were seen in those low-field breakdown devices, which were assumed to be due to the contamination in the thin films. Although the fabrication parameters were well controlled to eliminate the possible variations on processing each device, the performance of each device still exhibited variation. The degradation mechanisms of ac TFEL devices have been investigated and the fabrication process has also been reviewed to find out the responsible reasons for the device failure. Generally, the degradation (or failure mode) can be classified into three categories: Ag electrode delamination, dielectric breakdown, and field-induced chemical reaction.

Ag electrode delamination: Micrographs of the surface morphology of failed devices have been studied by using scanning electron microscopy (SEM). Figures 21 and 22 show the SEM micrographs of a device which exhibited

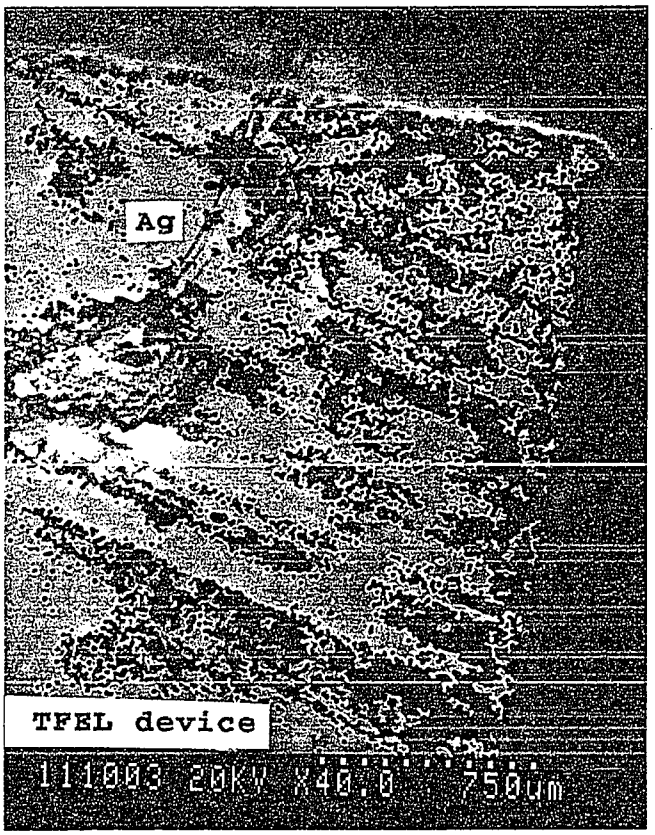

Figure 21. SEM micrograph of a failed TFEL device showing the top Ag electrode peeling off from the device.

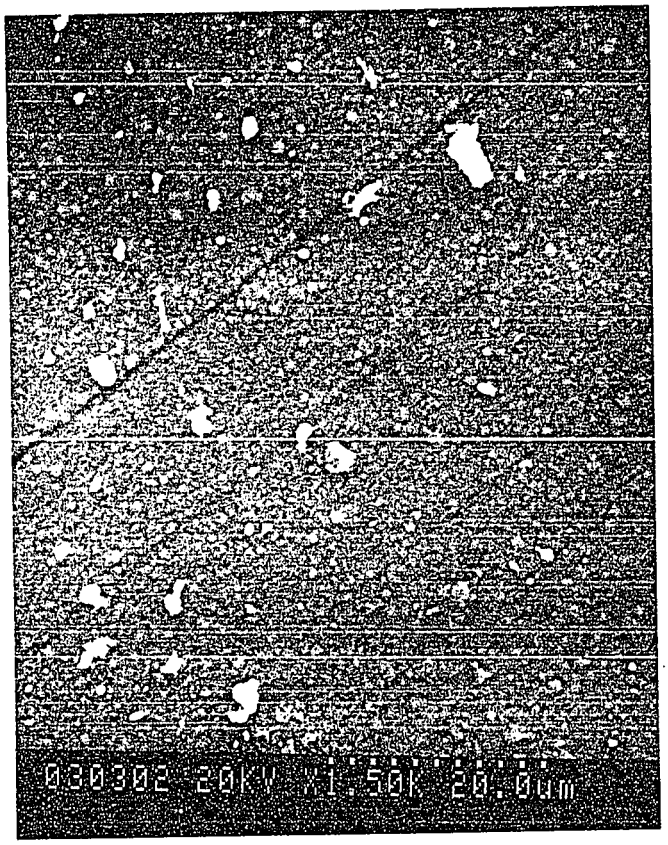

Figure 22. SEM micrograph showing the scratches and debris created on silicon nitride thin film.

breakdown under continuous applied voltage operation. From Figure 21, apparently, the top Ag electrode of the device peels off in parallel stripes. These parallel lines are believed to be due to scratches created on the silicon nitride film during the fabrication. As mentioned earlier, silicon nitride was deposited over the entire ITO substrate. Then photolithography was applied to selectively remove part of the nitride, at the edge of the substrate, to expose ITO electrode. Q-tips were used to spread photoresist on top of silicon nitride film in certain areas. This was done because it did not require a mask step, and we did not think the glass substrate could fit in the spinner. These Q-tips-created scratches, as shown in Figure 22, were left on the silicon nitride film after removal of the photoresist.

These areas later could create voids or trap contaminants when Ag was evaporated onto the silicon nitride film to form the electrodes. It was found that any voids or contaminants formed between the Ag electrode and underlying silicon nitride thin film could result in electrical arcs between electrodes and thermal destruction. In addition, any weakened area caused by poor adhesion in the insulator and Ag electrode would be ripped apart by the electrostatic forces between the trapped charge and the applied voltage, as seen in Figure 23. Water would also be ionized in the film by the high field.

Dielectric breakdown: Another breakdown mechanism is due to the dielectric breakdown. As shown in Figure 23, a number of craters are found in the silicon nitride insulating layer of failed devices. Breakdown in the insulating layers is believed to begin with an initiating event due to defects which can result from inhomogeneities in the insulating layers such as pinholes, cracks, or scratches.[72] As mentioned earlier, some scratches were created on the Si_3N_4 film surface during the fabrication process. These areas could create voids or trap contaminants when the Ag electrode was evaporated onto the silicon nitride film. Such defects could cause a local increase in the electric field and conductivity which would reduce the local dielectric strength and lead to breakdown. The electric field in the sandwich structure is about 2 to 3 MV/cm, as can be calculated directly from the applied voltage and total thickness of the sandwich structure. In other words, a conducting channel is formed in the insulating layer. The insulator then discharges itself through the channel, generating sufficient heat to evaporate the insulator. The breakdown event ends when the field across the insulator is insufficient to sustain the discharge when the breakdown region becomes open circuited, as the craters seen in Figure 23.

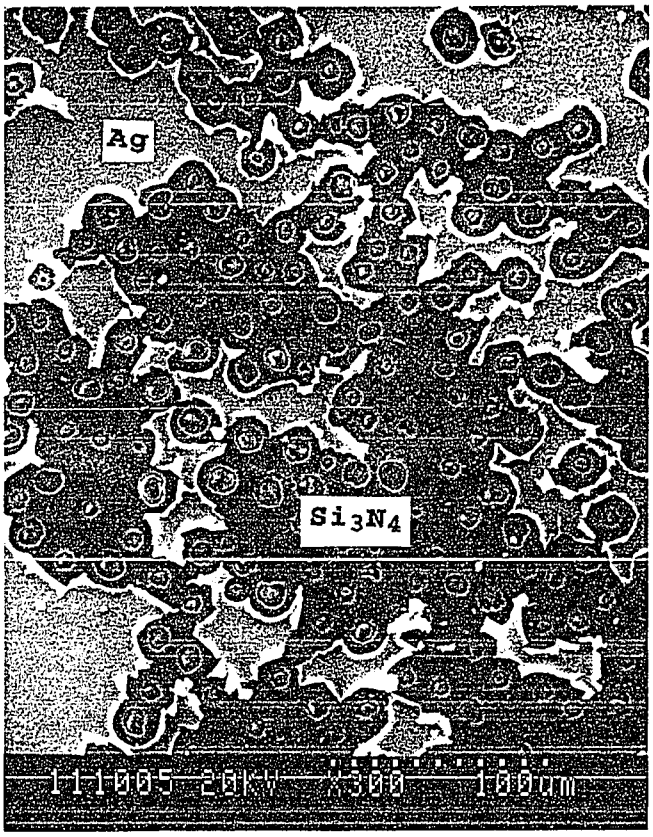

Figure 23. SEM micrograph of a device after dielectric breakdown, showing the severely damaged region of the PECVD fabricated silicon nitride dielectric.

Field-Induced Chemical Reaction: During high electric field operation in the atmosphere, chemical reaction can be induced by the electric field. ZnS is thermodynamically unstable,[73] thus zinc-oxy-sulfides can be simply formed under the given kinetic conditions. Because zinc-oxy-sulfides exhibit insulating behavior,[74] the formation of these new insulating layers may lower the applied electric field in the ZnS:Mn phosphor layer and contribute to the performance degradation of TFEL devices.

Future work:

The fabrication of good ac thin-film electroluminescent devices is achievable once the previous obstacles are overcome. The preparation must include very clean surfaces for each thin film and a moisture-controlled deposition process. Specifically, a suggested procedure for future work at SJSU is: (1) set up a particle-controlled environment, such as a clean room, around the working place of MOCVD system, and move the vacuum evaporator into that area; (2) keep the devices in a desiccator at all times when they are not used; (3) operate the devices under such a clean environment.

In addition, the phosphor and insulating materials must be of high purity, and the thickness of the layers must be

precisely controlled. Mechanical stress or scratching of the layers must be avoided, by adding a lithography step to remove photoresist. Another suggestion is to try different insulators as described in section 2.4, perhaps using a stacked structure to improve the lifetime of the devices.

Entirely, a well controlled impurity and moisture fabrication process is thought to be the most effective way to improve the short lifetime problem occurred in our studies.

6. CONCLUSION

ZnS:Mn thin-film electroluminescent (TFEL) devices using PECVD silicon nitride films as insulators have been fabricated and investigated. Some of our devices show very steady B-V and I-V characteristics. The performance reproducibility of TFEL devices is good. The threshold voltage was found to be in the range of 200 to 285 rms volts. Aging and memory effect were also observed in our devices. The most serious problem on the performance of our devices is the short lifetime. The longest lifetime was found to be three hours. The degradation mechanisms of ZnS:Mn TFEL devices have been considered. It was found that from SEM micrographs of the failed devices, the possible degradation mechanisms can be generally classified into three categories. They are Ag electrode delamination, dielectric breakdown, and field-induced chemical reaction. To improve the short lifetime problem, using other insulators with better dielectric properties is suggested. A stacked insulating structure is also recommended for future work. In addition, a clean and moisture-controlled fabrication environment to reduce the impurity content is strongly recommended.

7. REFERENCES

1. D. Z. Chuang, Materials Engineering Master Thesis Project. San Jose State University, 1992.

2. G. Destriau, "Research into the Scintillations of Zinc Sulfides to Alpha Rays," J. Chem. Phys., vol.33, 1936, p.620.

3. S.V. Petertyl and P.R. Fuller, "Improved Contrast and Visibility for Electroluminescent Displays," 18th Annual National Aerospace Electronics Conference, Dayton, Ohio, 16-18 May 1966.

4. S.V. Petertyl, "Development of High Contrast Electroluminescent Displays," Air Force Flight Dynamics Laboratory Report AFFDLTR-66-183, March 1967.

5. D. Kahng, "Electroluminescence of Rare-Earth and Transition Metal Molecules in II-VI Compounds via Impact Excitation," Appl. Phys. Lett., vol.13, 1968, p.210

6. T. Inoguchi, M. Takeda, Y. Kakihara, Y. Nakata and M. Yoshida,"Stable High-Brightness Thin-Film Electroluminescent Panels," S.I.D. Int. Symp. Dig. Tech. Papers, 1974, p.84.

7. S. Mito, C. Suzuki, Y. Kanatani and M. Ise, "TV Imaging System Using Electroluminescent Panels," S.I.D. Int. Symp. Dig. Tech. Papers, 1974, p.86.

8. S.Tanka, H. Deguchi, Y. Mikami, M. Shiiki and H. Kobayashi, "Red and Blue Electroluminescence in Alkaline-Earth Sulfide Thin-Film Devices," S.I.D. Int. Symp. Dig. Tech. Papers, 1986, p.29.

9. H. Xian, G. Zhong, S. Tanaka and H. Kobayashi, "Electroluminescence and Photoluminescence in Eu-Doped SrS Thin-Films," Jpn. J. Appl. Phys., vol.28, 1989, L1019.

10. S. Okamoto, E. Nakazawa and Y. Tsachiya, "Electroluminescence of SrS Thin Films Activated with Nd^{3+}, Sm^{3+}, Dy^{3+}, Ho^{3+}, and Er^{3+} Ions," Jpn. J. Appl. Phys., vol.28, 1989, p.406.

11. V. Shanker, S. Tanka, M. Shiiki, H. Deguchi, H. Kobayashi and H. Sasakura, "Electroluminescence in Thin-Film CaS:Ce," Appl. Phys. Lett., vol.45, 1984, p.960.

12. S. Tanka, V. Shanker, M. Shiiki, H. Deguchi and H. Kobayashi, "Multicolor Electroluminescent ZnS Thin Films Doped with Rare Earth Fluoride," Proc. Soc. Inf. Disp., vol.26, 1985, p.255.

13.G.H. Dieke and H.M. Crosswhite, Appl. Optics, vol.2, 1963, p.675.

14.T. Suyama, K. Okamoto and Y. Hamakawa, "New Type of Thin-Film Electroluminescent Device Having A Multilayer Structure," Appl. Phys. Lett., vol.41, 1982, p.462.

15.D.C. Morton and F. Williams, "An Electroluminescent Display Based on Spatial Separation of Hot-Electron Generation and Luminescent Excitation in Multilayer Films," Proc. Soc. Inf. Disp., vol.23, 1982, p.91.

16.G. Smarte and N.M. Baran, "Face to Face," BYTE, vol.13, 1988, p.243.

17.R.V. Stroh and B. Dolinar, "Lighting the Way," BYTE, vol.13, 1988, p.275.

18.G.M. Robinson, "Display System Leap Forward," Design News, vol.45, 1989, p.53.

19.P. Pleshko, "AC Electroluminescent Display Technology: Challenges and Potential," Proc. Soc. Inf. Disp., vol.32, 1991, p.105.

20.J.L. Vossen, Physics of Thin Films, vol.9, Academic Press, 1977.

21.W.E. Howard, "The Importance of Insulator Properties in a Thin Film Electroluminescent Device," IEEE Trans. Electron Devices, vol.ED-24, 1977, p.903.

22.D.A. Cusano, "Luminescence of Organic and Inorganic Materials, Wiley, New York, 1962.

23.D.C. Krupa, "Hot-Electron Impact Excitation of Tb3+ Luminescence in ZnS:Tb3+ Thin Films," J. Appl. Phys., vol.43, 1972, p.426.

24.J. Shah and A.E. Digiovanni, "AC Electroluminescence in Thin-Film ZnSe:Mn," Appl. Phys. Lett., vol.33, 1978, p.995.

25.D.C. Morton and F. Williams, "A New Thin-Film Electroluminescent Material-ZnF_2:Mn," Appl. Phys. Lett., vol.35, 1979, p.671.

26.S.L. McCarthy and J. Lambe, "Thin-Film Electroluminescence in Impurity-Doped Al_2O_3," Appl. Phys. Lett., vol. 37, 1980, p.554.

27.T. Inoguchi and S. Mito, Topics in Applied Physics: Electroluminescence, Springer-Verlag Berlin Heidelberg, vol.17, 1977, p.197.

28.R. Mach and G.O. Muller, "Physical Concepts of High-Field, Thin Film Electroluminescence Devices," Phys. Stat. Sol.(A), vol.69, 1982, p.11.

29.L.E. Trannas, Flat Panel Displays and CRTs: Electroluminescence, Van Nostrand Reinhold Company Inc., 1985.

30.S. Tanka, H. Kobayashi, H. Saskura and Y. Hamakawa, "Evidence for the Direct Impact Excitation of Mn Centers in Electroluminescent ZnS:Mn Films," J. Appl. Phys., vol.47, 1976, p.5391.

31.P.M. Alt, "Thin-Film Electroluminescent Displays: Device Characteristics and Performance," Proc. Soc. Inf. Disp., vol.25, 1984, p.123.

32.K.A. Neyts and P. De Visschere, "Analytical Model for Thin Film Electroluminescent Devices," J. Appl. Phys., vol.68, 1990, p.4163.

33.J. Watanabe, M. Wakitani, S. Sato and S. Miura,"Analysis of Deterioration in Brightness-Voltage Characteristics," S.I.D. Int. Sym. Dig. Tech. Papers,1987, p.288.

34.M. Nishikawa, T. Matsuoka, T. Tohda, Y. Fujita, J. Kuwata and A. Abe, "A High Stable TFEL Panel with CaS Buffer Layer," S.I.D. Int. Sym. Dig. Tech. Papers, 1988, p.19.

35.M. Yoshida, Y. Kakihara, T. Yamashita, K. Taniguchi and T. Inoguchi, "The Mechanism of Inherent Memory in Thin Film EL device," Jpn. J. Appl. Phys., 1978, Suppl.17-1 p.127.

36.W.E. Howard, O. Sahni and P.M. Alt, "A Simple Model for the Hysteretic Behavior of ZnS:Mn Thin Film Electroluminescent Devices," J. Appl. Phys., vol.53, 1982, p.639.

37.K.C. Yang, S. John and T. Owen, "Mechanisms of Negative Resistance Characteristics in AC Thin Film Electroluminescent Devices," IEEE Trans. Electron Devices, vol.ED-30, 1983, p.452.

38.G.O. Muller and R. Mach, "Physics of Electroluminescent Devices," J. of Luminescence, vol.40,41, 1988, p.92.

39.S.K. Tiku and G.C. Smith, "Choice of Dielectric for TFEL Displays," IEEE Trans. Electron Devices, vol.ED-31, 1984, p.105.

40.P.M. Alt, D.B. Dove and W.E. Howard, "Experimental Results on the Stability of AC Thin Film Electroluminescent Devices," J. Appl. Phys., vol.53, 1982, p.5186.

41.H. Kozawaguchi, B. Tsujiyama and K. Murase, "Thin-Film Electroluminescent Device Employing Ta2O5 RF Sputtered Insulating Film," Jpn. J. Appl. Phys., vol.21, 1982, p.1028.

42.S.K. Tiku and S.H. Rustomji, "Dielectrics for Bright EL Displays," IEEE Trans. Electron Devices, vol.ED-36, 1989, p.1947.

43.Y. Sano, K. Nunomura, N. Koyama, H. Sakuma and K. Utsumi, "A Novel TFEL Device Using a High-Dielectric-Constant Multilayer Ceramic Substrate," Proc. Soc. Inf. Disp., vol.27, 1986, p.169.

44.S. Takata, T. Minami and T. Miyata, "Crystallinity of Emitting Layer and Electroluminescence Characteristics in Multicolor ZnS Thin Film Electroluminescent Device with a Thick Dielectric Ceramic Insulating Layer," Thin Solid

Films, vol.193, 1990, p.481.

45.T. Minami, T. Miyata, S. Takata and I. Fukuda,"High-Luminance Green Zn2SiO4:Mn Thin Film Electroluminescent Devices Using an Insulating BaTiO3 Ceramic Sheet," Jpn. J. Appl. Phys., vol.30, 1991, p.L117.

46.R.C.G. Swan, R.R. Mehta and T.P. Cauge, "The Preparation and Properties of Thin Film Silicon-Nitrogen Compounds Produced by a Radio Frequency Glow Discharge Reaction," J. Electrochem., vol.114, 1967, p.713.

47.A. Vecht, "A Review of Electroluminescent Thin-Film Fabrication Techniques," S.I.D. Int. Symp. Dig. Tech. Papers, 1989, p.304.

48.A.Vecht and A. Saunders, Electrochem. Soc. Extended Abstracts, vol.87.2, 1987, p.1685.

49.Tannas, Flat Panel Display and CRTs, Van Nostrand Reinhold Company Inc., 1985.

50.Z.K. Kun, D. Leksell, D.R. Malmberg, J. Murphy and L.J. Sienkiewicz, "Influence of Chlorine on the Crystal Structure and Electroluminescent Behavior of ZnS:Mn Films in Thin-Film Electroluminescent Devices," J. Electronic

Mats., vol.10, 1981, p.287.

51.P. Thioulouse, R. Tueta, A. Izrael and N. Duruy, "The Effect of Post-Deposition Annealing upon the Electro-Optical Characteristics and the Microstructure of ZnS:Mn ACTFEL Devices," Proc. Soc. Inf. Disp., vol.26, 1985, p.223.

52.M. Nishikana, T. Matsuka, T. Tohda, Y. Fujita, J. Kunata and A. Abe, "A High Stable TFEL Panel with CaS Buffer Layer," S.I.D. Int. Symp. Dig. Tech. Papers, 1988, p.19.

53.T. Suntola et al. "Atomic Layer Epitaxy for Producing EL Thin Films," S.I.D. Int. Symp. Dig. Tech. Papers, 1980, p.109.

54.J. Dunker, S.I.D. Int. Symp. Dig. Tech. Papers, 1983, p.42.

55.R.T. Tuenge, "Thin Film Electroluminescent Phosphors for Patterned Full-color Display," Springer Proceedings in Physics: Electroluminescence, vol.59, 1982, p.148.

56.M. Pena, R. Makela, and T. Suntola, "Characterization of Surface Exchange Reactions Used to Grow Compound Films," Appl. Phys. Letters, vol.38, 1981, p.131.

57. P.J. Wright and B. Cockayne, "The Organometallic Chemical Vapor Deposition of ZnS and ZnSe at Atmospheric Pressure," J. Crystal Growth, vol.59, 1982, p.148.

58. A.F. Cattell, B. Cockayne, K. Dexter, J. Kirton, and P. Wright, "Electroluminescence from Films of ZnS:Mn Prepared by Organometallic Chemical Vapor Deposition, IEEE Trans. Electron Devices, vol.ED-30, 1983, p.471.

59. K. Kirabayashi and O. Kogure, "AC Thin Film ZnS:Mn Electroluminescent Device Prepared by Metal Organic Chemical Vapor Deposition," Jpn. J. Appl. Phys., vol.24, 1985, p. 1484.

60. T. Minami, T. Miyata, K. Kitamura, H. Namto, and S. Takata, "Low Voltage Driven MOCVD-Grown ZnS:Mn Thin-Film Electroluminescent Devices Using Insulating BaTiO3 Ceramic Sheets," Jpn. J. Appl. Phys., vol.27, 1988, p.L876.

61. T. Miyata, T. Minami, and S. Takata, "Influence of Mn Doping Conditions on Electroluminescent Characteristics of ZnS:Mn Thin Film Electroluminescent Devices Using Insulating Ceramic," J. Crystal Growth, vol.117, 1992, p.1021.

62.M.I. Abdalla, J.L. Plumb, and L.L. Hope, S.I.D. Sym. Dig. Tech. Papers, 1984, p.5.

63.A. Saunder and A. Vecht, "The Role of Chemical Vapor Deposition in the Fabrication of High Field Electroluminescent Displays," Springer Proceedings in Physics: Electroluminescnece, vol.38, 1989, p.210.

64.P.J. Wright, B. Cockayne, A.F. cattell, P.J. Dean, A.D. Pitt and G.M. Blackmore, "Variation in the Luminescent and Structural Properties of Sputter-Deposited ZnS:Mn Thin Films with Post-Deposition Annealing," J. Crystal Growth, vol.59, 1982, p.155.

65.K. Kirabayashi and H. Kozawaguchi, "ZnS:Mn Electroluminescent Device Prepared by Metal-Organic Chemical Vapor Deposition," Jpn. J. Appl. Phys., vol.25, 1986, p.711.

66.Marc Jensen, Materials Engineering Senior Project San Jose State University, 1986.

67.Hoa Do, Materials Engineering Master Thesis Project San Jose State University, 1988.

68.L.I. Maissel and R. Glang, Handbook of Thin Film Technology, Mcgraw-Hill Inc., New York, 1970, pp.1-33.

69."Powder Diffraction File Search Manual for Common Phases," Swarthmore, Pa: JCPDS-International Center for Diffraction Data, 1981.

70.D.H. Smith, "Modeling ac Thin Film EL Device," J. of Luminescence, vol.23, 1981, p.209.

71.K.W. Yang and S.J.T. Owen,"Deep Traps and Mechanism of Device Aging in ACTFEL Devices," Proc. Soc. Inf. Disp., vol.25,1984, p.7.

72.N. Klein,"A Theory of Localized Electronic Breakdown in Insulating Films," Adv. Phys., vol.21, 1972, p.605.

73.P.W. Alexander, C. Sherhod and M.J. Stowell, "Forming of Power DC Electroluminescent Displays:II. Mechanism and Implications for Maintenance," J. Phys., vol.21, 1988, p.1635.

74.T. Matsuoka, J. Kuwata, M. Nishikawa, Y. Fujita, T. Tohda and A. Abe, "Influence of Oxygen and Metal Oxide Impurities in ZnS:Mn Film on Characteristics of

Electroluminescent Devices," Jpn. J. Appl. Phys., vol.27, 1988, p.1426.

8. APPENDIX A. Design of the Shower Head

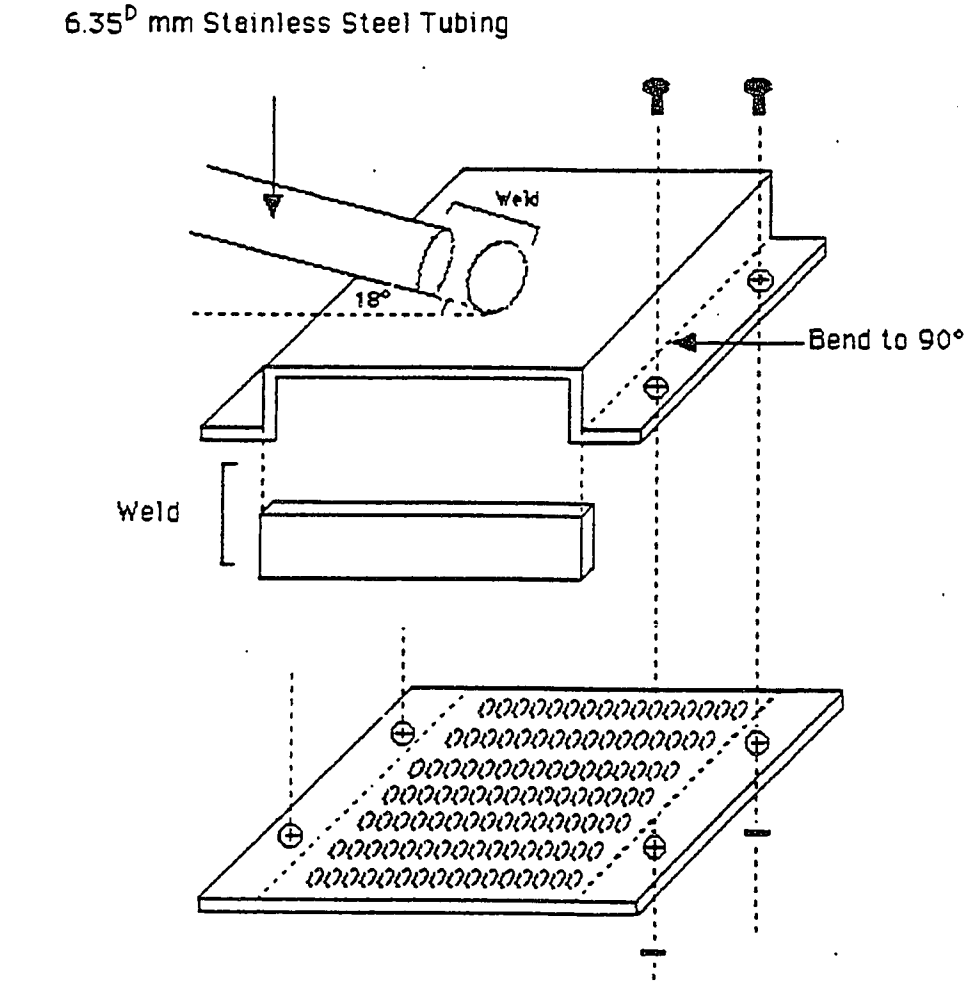

(a)

Figure 24. Assembly drawings of the shower head. (a) Schematic diagram of each component and the whole assembly graph of the shower head, (b) the finished shower head, (c) the side view of the finished shower head.

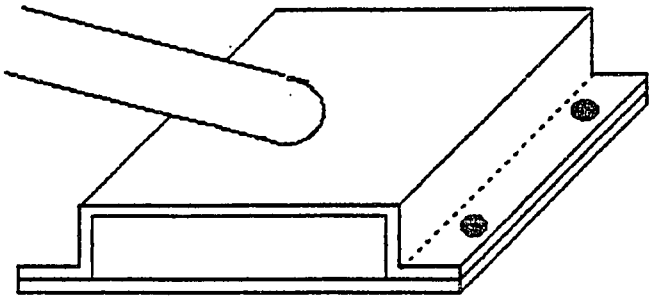

(b)

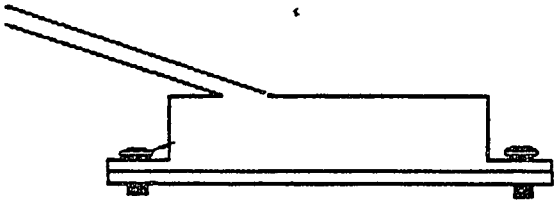

(c)